SAND2015-4757C

# A Comprehensive View of Gaseous Hydrogen-Assisted Cracking

Brian Somerday

Sandia National Laboratories, Livermore CA, USA

International Institute for Carbon-Neutral Energy Research ($I^2$CNER), Fukuoka, Japan

Eastern New York Chapter of ASM 2015 Spring Symposium
GE Global Research, Niskayuna, NY
May 19, 2015

# Design and materials selection for hydrogen fuel components must consider $H_2$-assisted cracking

## stationary and transport vessels
(martensitic steels)


## on-board tanks
(aluminum liners, stainless steel boss)

## pipelines
(ferritic steels)

## manifold components
(stainless steels)

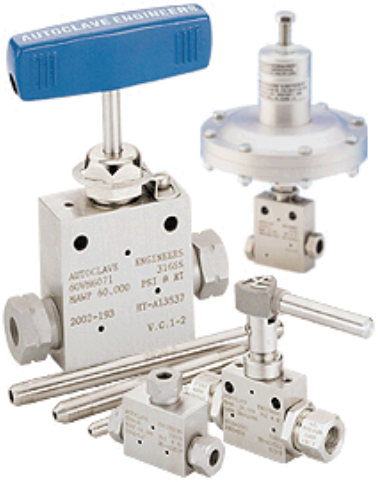


Sandia National Laboratories

# $H_2$-assisted cracking is multi-element phenomenon

## *Trends may be dominated by one element*

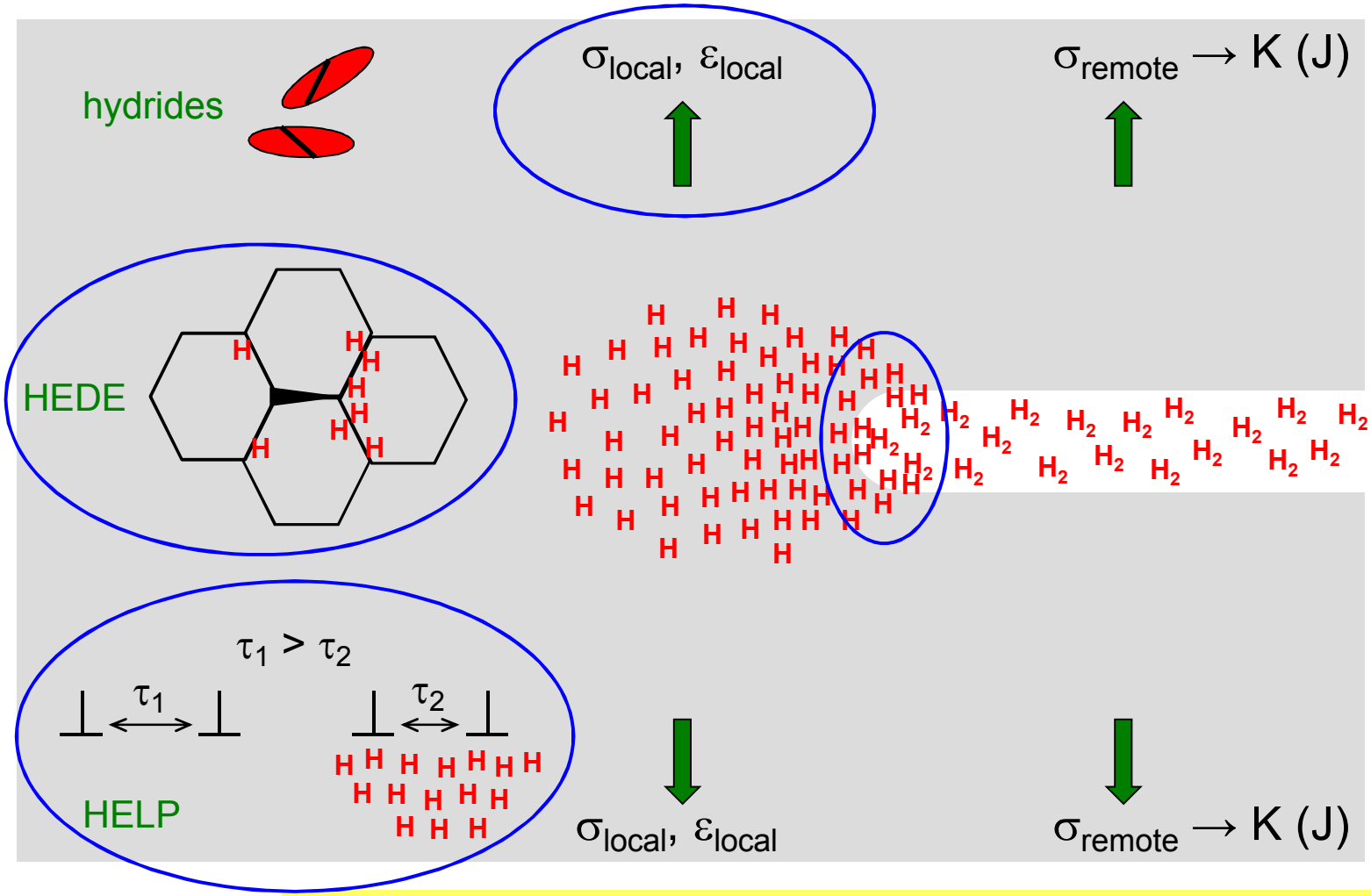


***Hydrogen-assisted cracking governed by crack-tip strain field***

Sandia National Laboratories

# *Issue-driven research goal*: measure $H_2$-assisted cracking thresholds for martensitic steels

K.A. Nibur et al., *Metall Mater Trans A*, 2013

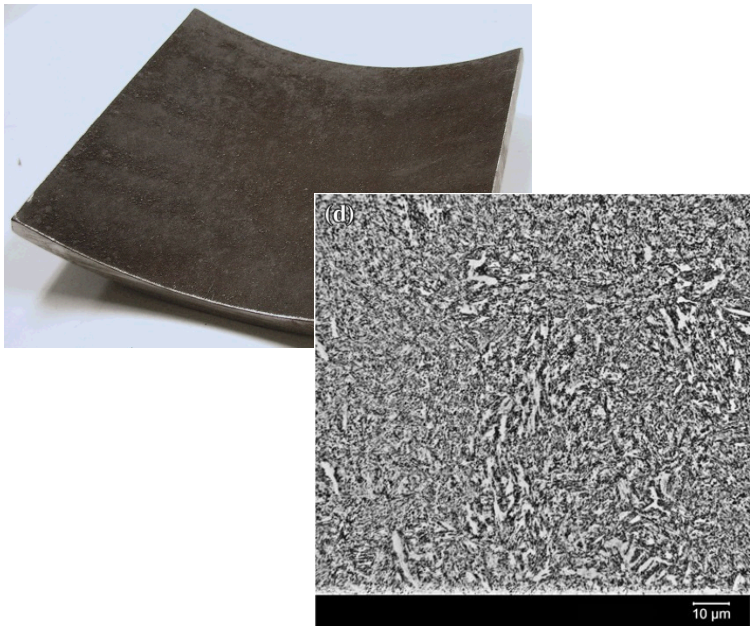


- **Material**
  - Cr-Mo(-Ni) pressure vessel steels
  - Yield strengths = 600 to 1050 MPa
- **Mechanical loading**
  - Constant displacement
  - Rising displacement = 0.05 mm/min (~3 MPa $m^{1/2}$/min)
- **Environment**
  - Supply gases: 99.9999% $H_2$
  - Pressure = 103 MPa (15,000 psi)
  - Room temperature

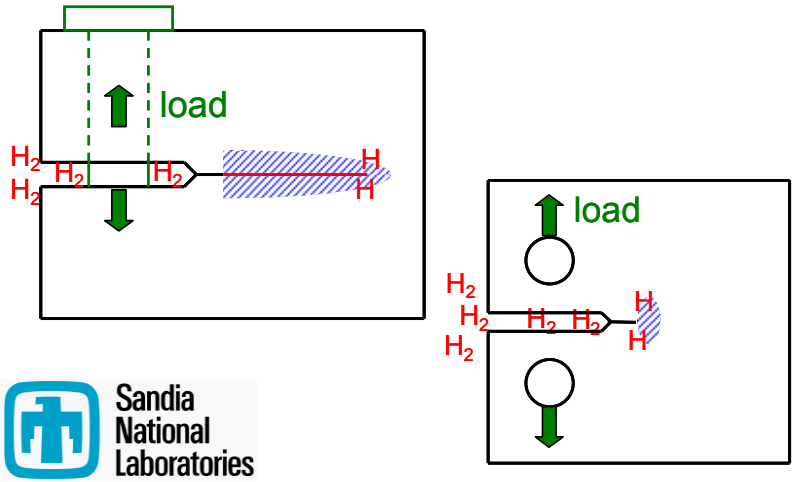


Sandia National Laboratories

# $H_2$-assisted cracking thresholds measured using two conventional methods

K.A. Nibur et al., *Metall Mater Trans A*, 2013

constant displacement method: "arrest" threshold, $K_{THa}$

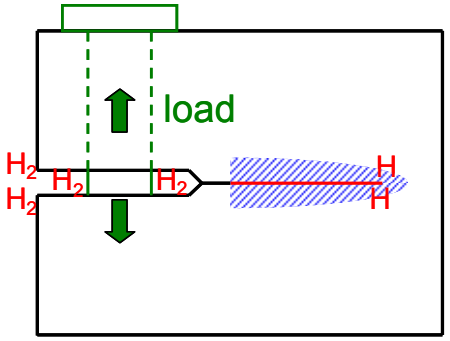


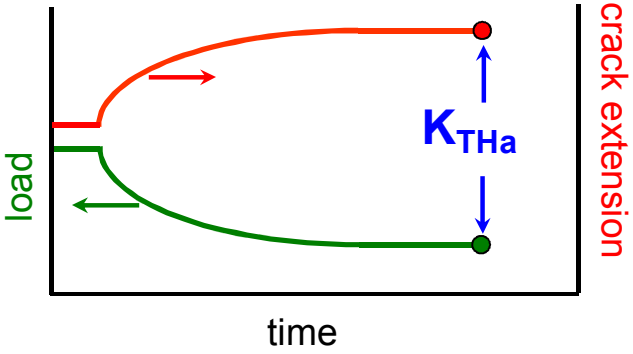


rising displacement method: "initiation" threshold, $K_{THi}$

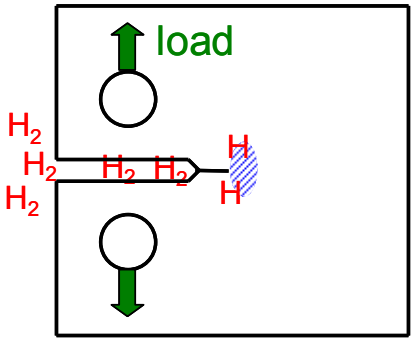


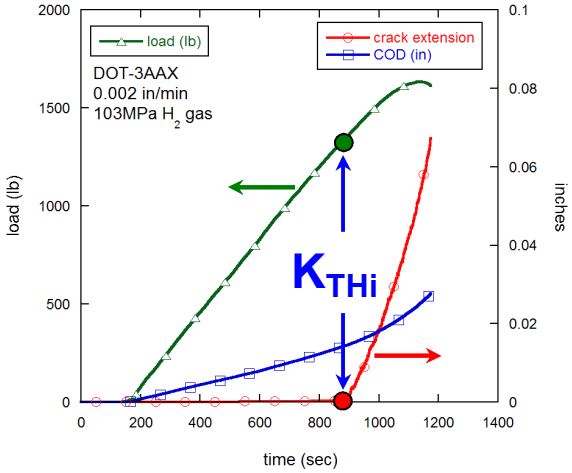


***Key difference in test methods: propagating crack vs. stationary crack***

Sandia National Laboratories

# Crack arrest thresholds ($K_{THa}$) higher than crack initiation thresholds ($K_{THi}$) at lower $\sigma_{YS}$

K.A. Nibur et al., *Metall Mater Trans A*, 2013

pressure vessel steels

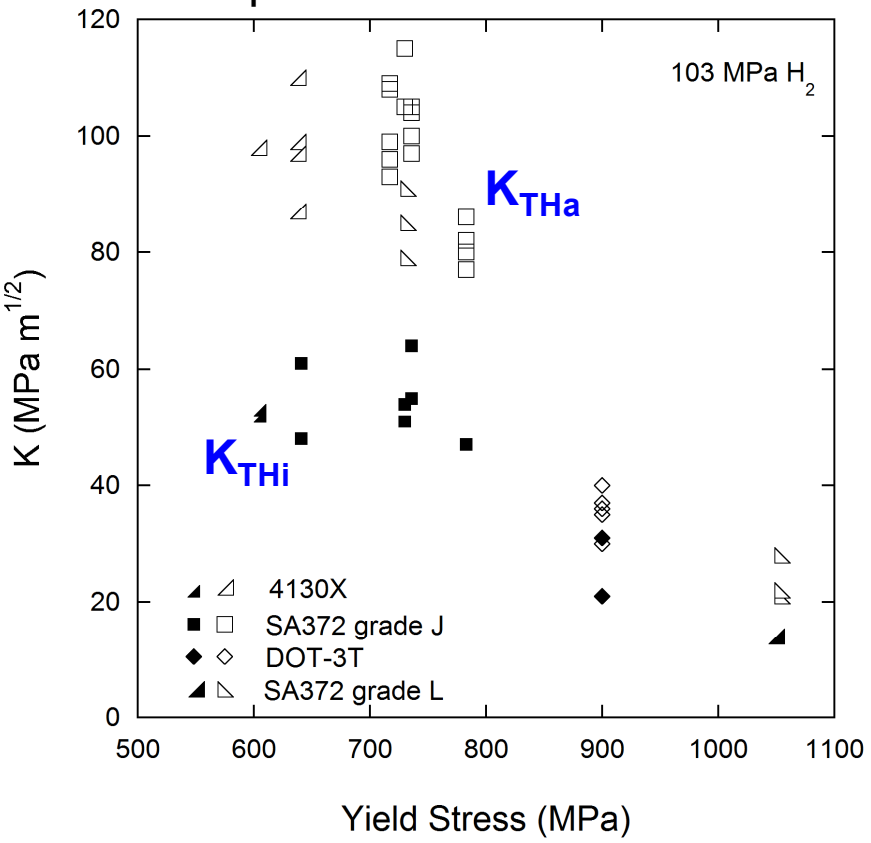


4130X pressure vessel steel

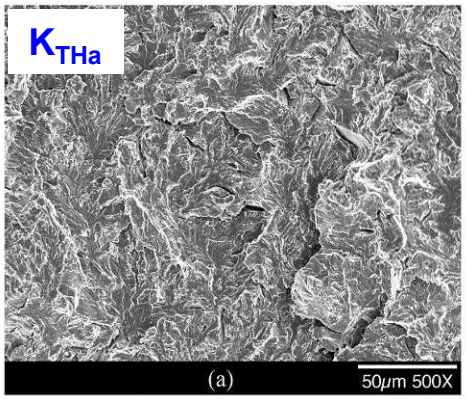


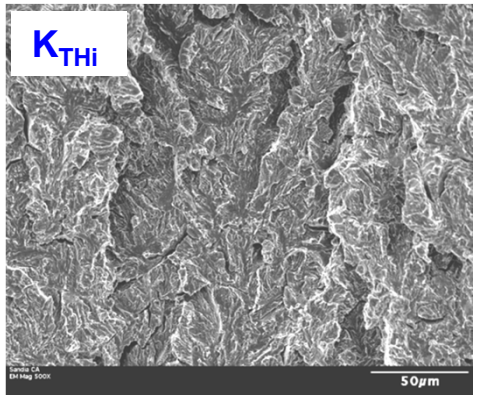


- ***Divergent thresholds not attributed to difference in fracture mechanism***
- ***Assume fracture mechanism is strain-controlled, i.e., governed by $\varepsilon_{local}$***
  - ***Consistent with plasticity-related hydrogen-induced cracking (PRHIC)***

    Takeda and McMahon, *Metall Trans A*, 1981

***Can observed trends be rationalized based on crack-tip mechanics?***

Sandia National Laboratories

# Mechanics of propagating vs. stationary cracks illuminated by crack growth resistance curves

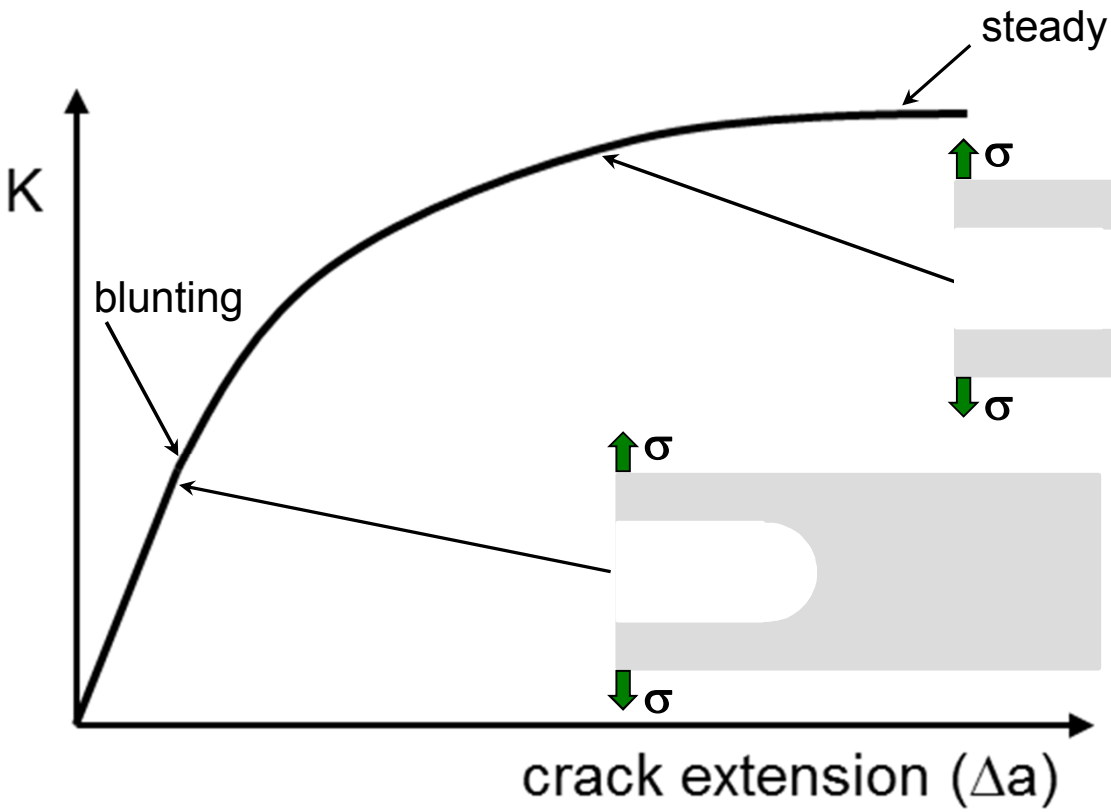


$$\varepsilon_{local}^{ss} \sim \ln\left(\frac{K^2}{r}\right)$$

Rice et al., *ASTM STP 700*, 1980

$$\varepsilon_{local} \sim \left(\frac{K^2}{r}\right)$$

Hutchinson; Rice and Rosengren, *J Mech Phys Solids*, 1968

***Crack-tip strain field weaker for propagating crack vs. stationary crack***

Sandia National Laboratories

# Weaker crack-tip strain field for propagating crack can account for higher crack-arrest thresholds

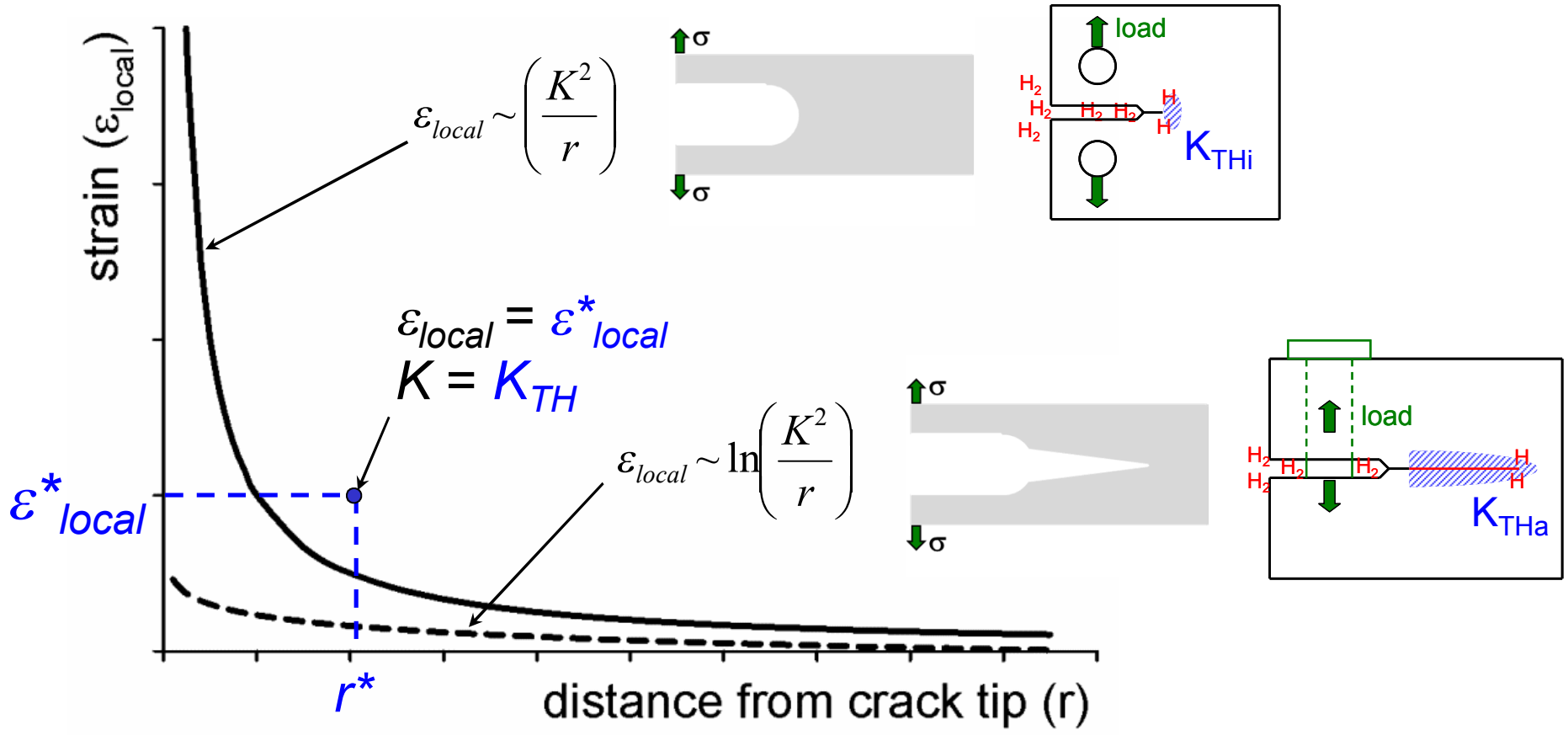


***Strain-controlled fracture criterion ($\varepsilon^*_{local}$) coupled with strain field amplitudes leads to $K_{THa} > K_{THi}$***

Sandia National Laboratories

# $K_{TH}$ vs. yield strength trends can be rationalized based on crack-tip mechanics framework

K.A. Nibur et al., *Metall Mater Trans A*, 2013

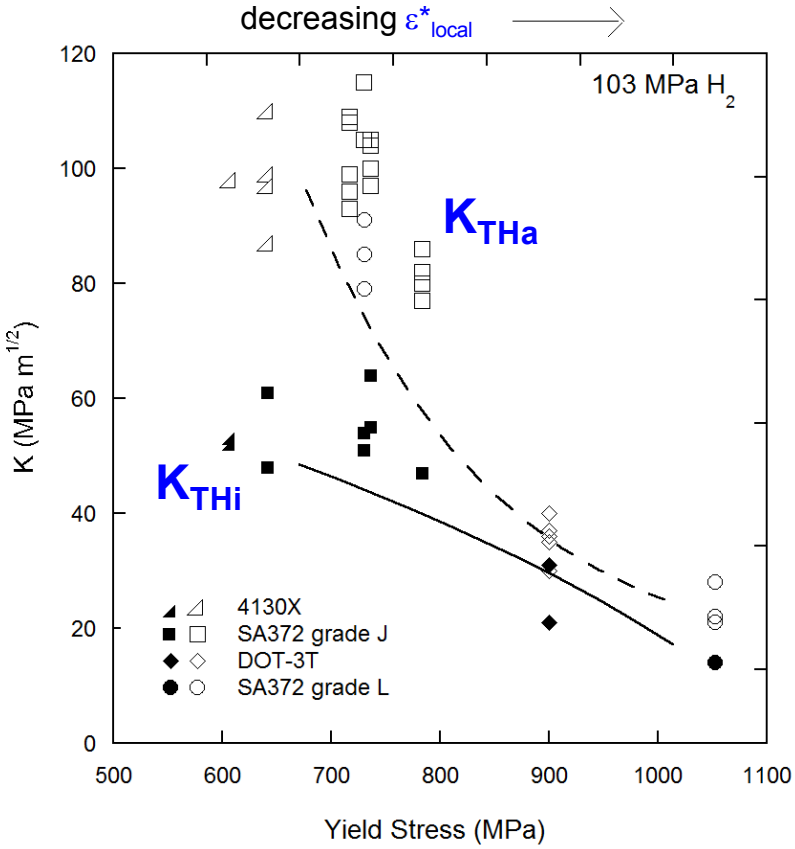


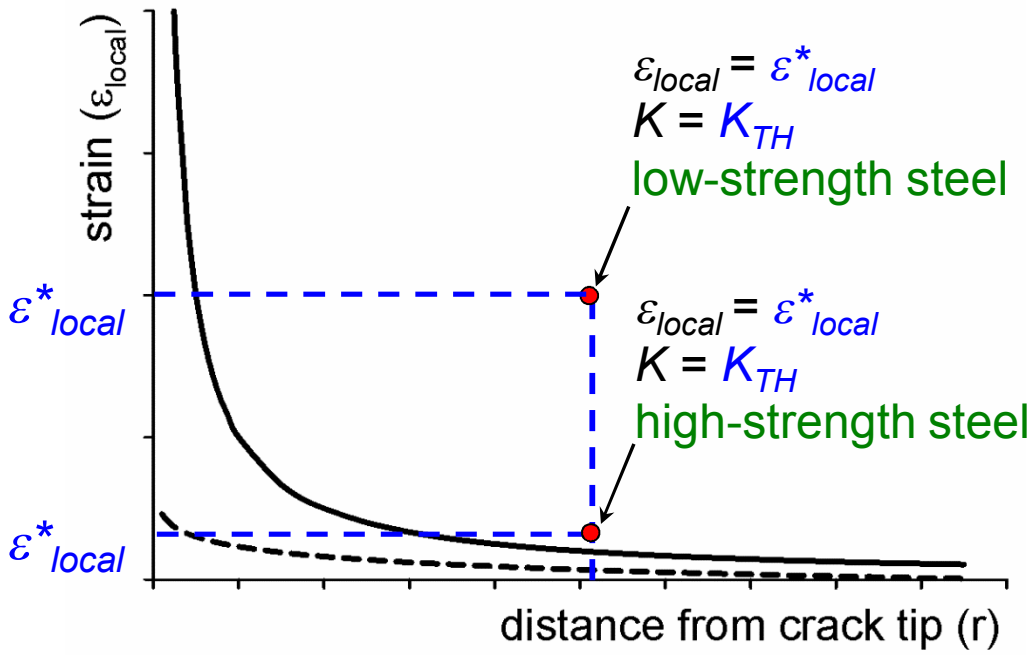


***Assumption that $\varepsilon^*_{local}$ decreases as yield strength increases can explain converging $K_{THa}$ and $K_{THi}$***

Sandia National Laboratories

# $H_2$-assisted cracking is multi-element phenomenon

## *Trends may be dominated by one element*

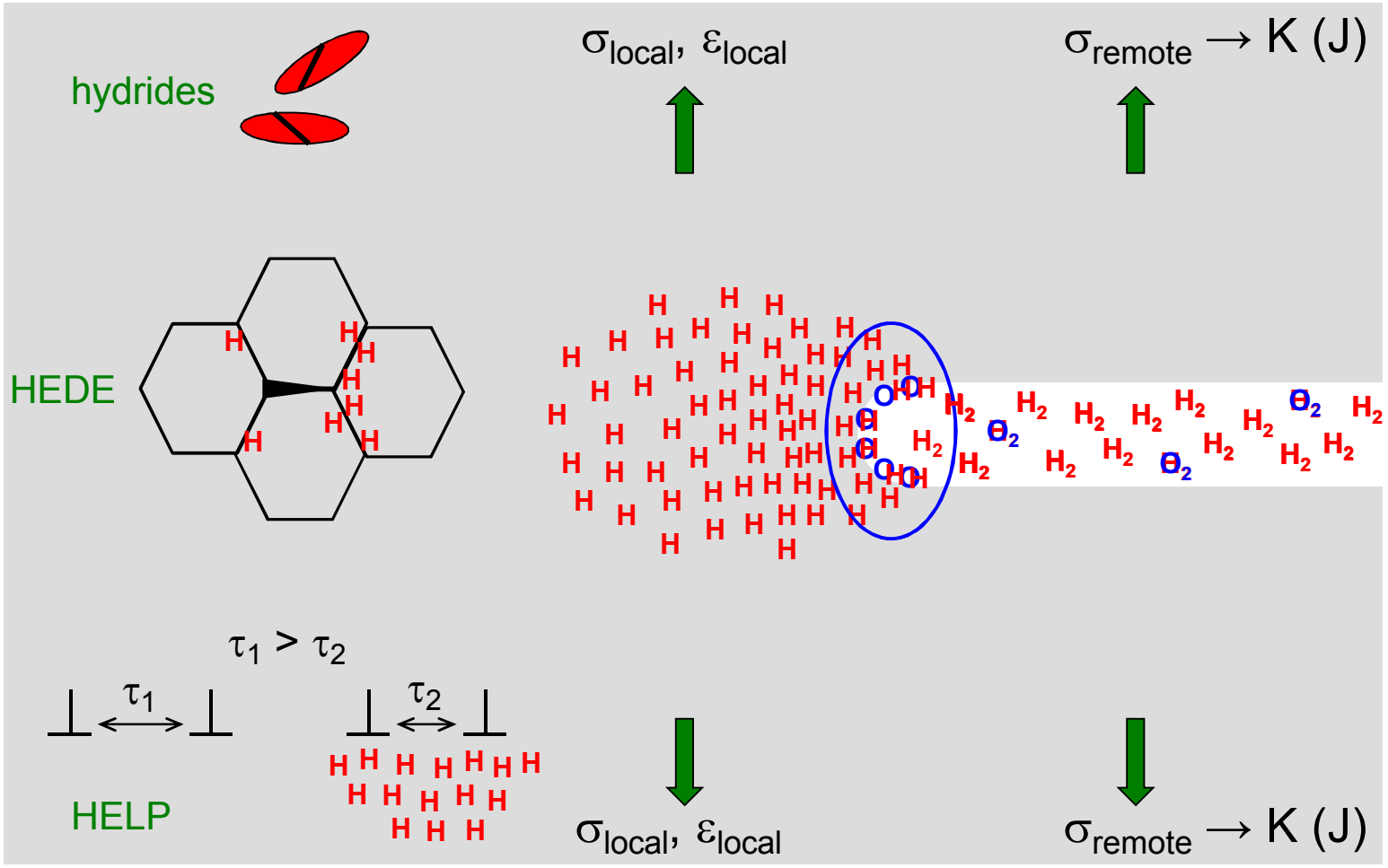


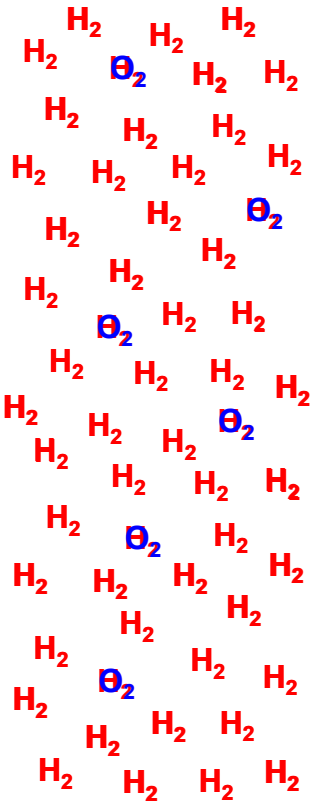

***Hydrogen uptake retarded by oxygen adsorption on crack-tip surface***

Sandia National Laboratories

# *Issue-driven research goal*: quantify $O_2$-modified, $H_2$-accelerated fatigue crack growth for pipe steel

B.P. Somerday et al., *Acta Mater*, 2013

- API 5L X52 steel composition

| C | Mn | P | S | Si | Cu | Ni | Cr | V | Nb | Al | CE |
|---|---|---|---|---|---|---|---|---|---|---|---|
| 0.06 | 0.87 | 0.011 | 0.006 | 0.12 | 0.03 | 0.02 | 0.03 | 0.002 | 0.03 | 0.034 | 0.11 |

- Tensile properties
  - Yield strength: 428 MPa
  - Ultimate tensile strength: 483 MPa

ferrite + 8 vol% pearlite

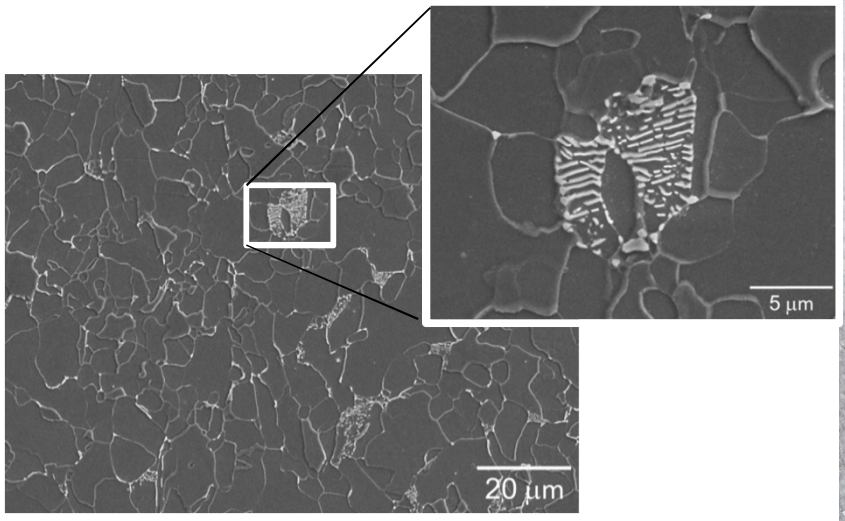



324 mm OD x 12.7 mm WT

Sandia National Laboratories

# Measured fatigue crack growth relationships for X52 steel in high-pressure $H_2$ with controlled $O_2$ levels

B.P. Somerday et al., *Acta Mater*, 2013

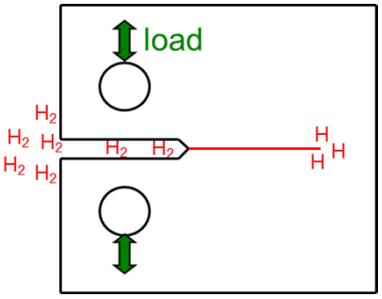


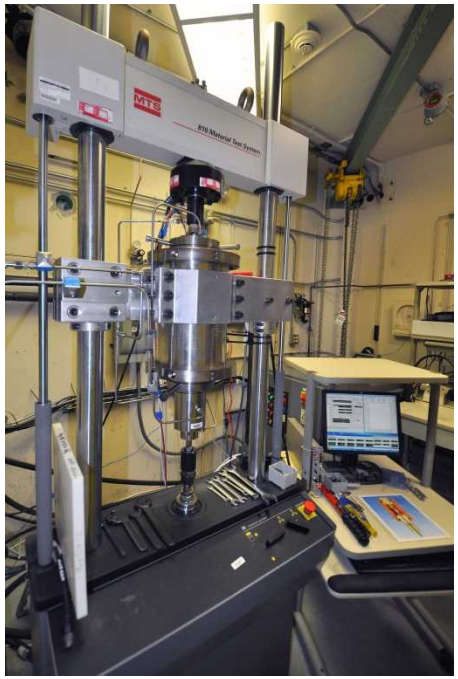

- **Material**
  - X52 ERW pipeline steel
- **Instrumentation**
  - Internal load cell in feedback loop
  - Crack-opening displacement measured internally using LVDT
  - Crack length calculated from compliance
- **Mechanical loading**
  - Triangular load-cycle waveform
  - Constant load amplitude or constant $\Delta K$
- **Environment**
  - Supply gases: 99.9999% $H_2$
    $H_2$ with 10-1000 vppm $O_2$
  - Pressure = 21 MPa (3,000 psi)
  - Room temperature

Sandia National Laboratories

# $H_2$-accelerated fatigue crack growth not absolutely inhibited by $O_2$: depends on da/dN and R ratio

B.P. Somerday et al., *Acta Mater*, 2013

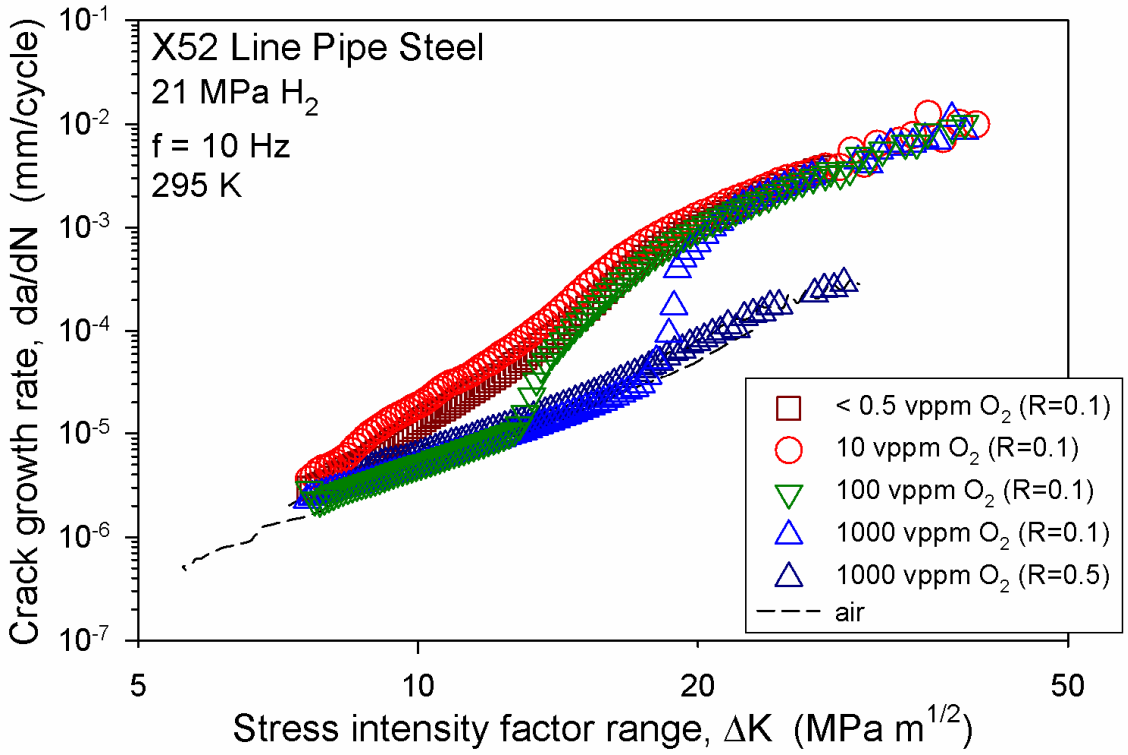


- At lower ΔK, crack growth rates in $H_2$ environments same as rates in air
- At R=0.1, hydrogen-accelerated crack growth observed at higher ΔK
  - da/dN at onset of hydrogen-accelerated crack growth depends on $O_2$ concentration
- At R=0.5, hydrogen-accelerated crack growth not observed

- ***Why is da/dN at onset of $H_2$-accelerated cracking a function of $O_2$ concentration?***
- ***Why does higher R promote inhibition?***

Sandia National Laboratories

# Central physical premise: oxygen adsorption at crack tip can inhibit H uptake

B.P. Somerday et al., *Acta Mater*, 2013

- Initial inert-environment crack growth modeled by blunting-resharpening
- Oxygen out-competes hydrogen for adsorption sites on freshly exposed crack-tip surface
- Extent of oxygen adsorption depends on crack-tip area, proportional to crack-growth increment (*da*)
  - when $da < da_{crit}$, crack tip *fully passivated* by oxygen
  - when $da > da_{crit}$, crack tip *not fully passivated* → H uptake
- Develop model that quantitatively relates adsorbed oxygen (H uptake) to mechanical and environmental variables

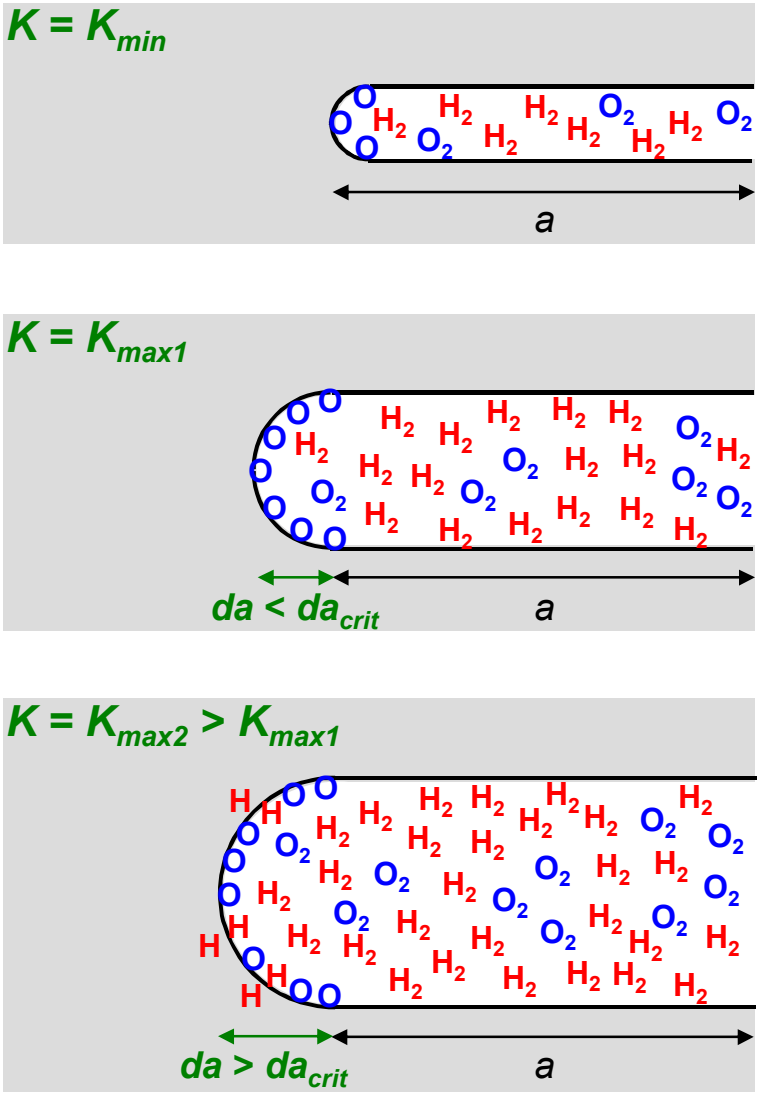


Sandia National Laboratories

# Model developed based on idealized crack geometry and diffusion-limited oxygen adsorption

- *Goal*: quantify amount of adsorbed oxygen (*n*) during load-cycle time ($\Delta t$)
- *Key assumption*: *adsorption rate-limited by $O_2$ diffusion in crack channel*
  - constant crack-channel height (*h*) during diffusion
  - steady state $p_{O2}$ profile
- Model foundation: oxygen delivered to crack tip ($Jh\Delta t$) = oxygen adsorbed on crack tip ($S\theta\pi\Delta a$)

$$J = \text{flux} = D\frac{\chi p_{tot}}{R_g T a^*}$$

$$h = \text{channel height} = 0.6(1-\nu^2)\frac{\sigma_0}{E}\left(\frac{\Delta K}{\sigma_0(1-R)}\right)^2$$

$$\Delta t = 1/f$$

$\theta$ = oxygen coverage  $S$ = surface site density

B.P. Somerday et al., *Acta Mater*, 2013

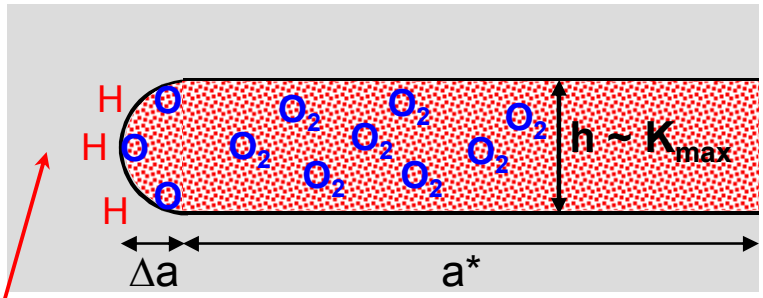


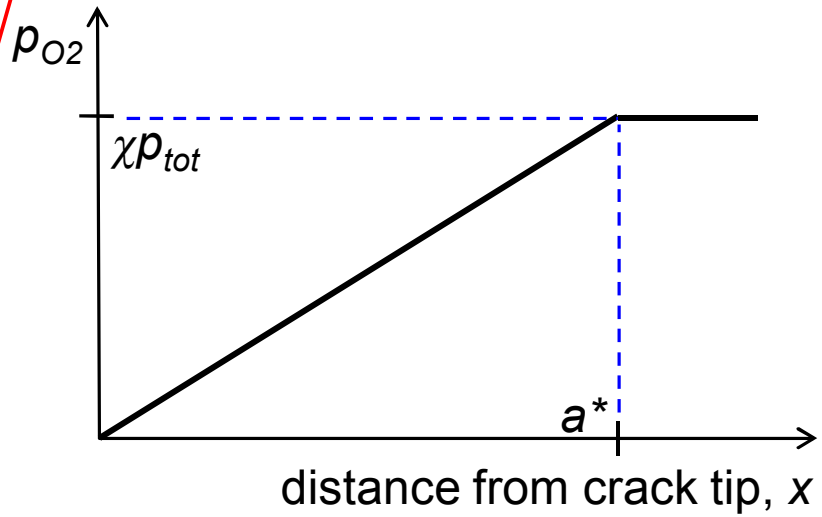


***H uptake and accelerated crack growth when $\theta = \theta_{crit}$***

$$(\Delta a) f\big|_{crit} = \frac{0.3\chi D p_{tot}(1-\nu^2)}{\pi S\theta_{crit} R_g T E \sigma_0}\left(\frac{\Delta K}{\sqrt{a^*}(1-R)}\right)^2$$

Sandia National Laboratories

# Model predictions consistent with da/dN vs. ΔK data measured in $H_2$+$O_2$ gas at R = 0.1 and 0.5

B.P. Somerday et al., *Acta Mater*, 2013

$$\Delta a_{crit} = \frac{0.3\chi D p_{tot}(1-\nu^2)}{f\pi S\theta_{crit} R_g T E \sigma_0}\left(\frac{\Delta K}{\sqrt{a^*}(1-R)}\right)^2$$

assume $\Delta a \sim da/dN$

$S\theta_{crit}$ calculated from measured da/dN at onset of accelerated crack growth for $H_2$+100 vppm $O_2$

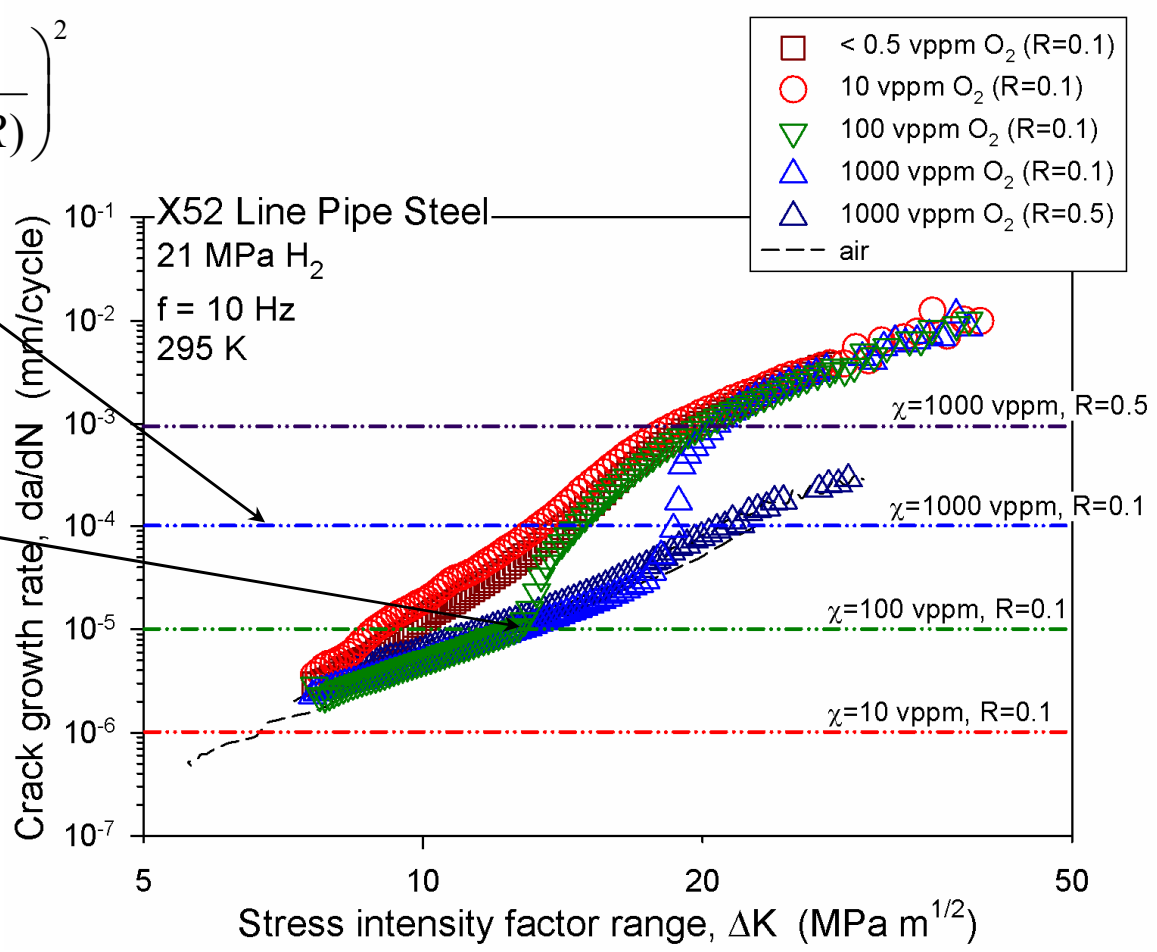


***Favorable correlation between measurements and model gives credence to physical assumptions***

Sandia National Laboratories

# Establishing physical description allows rationalization of $O_2$ concentration and R ratio effects

- $O_2$ concentration ($\chi$) → affects gradient in crack channel
- R ratio → affects height of crack channel

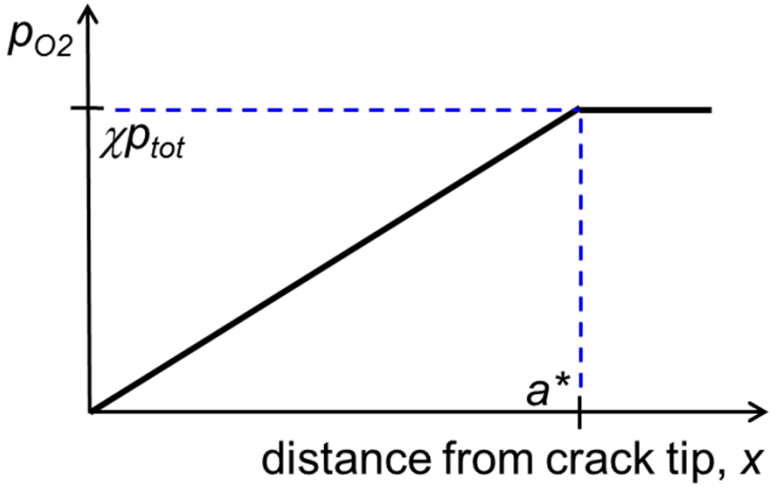


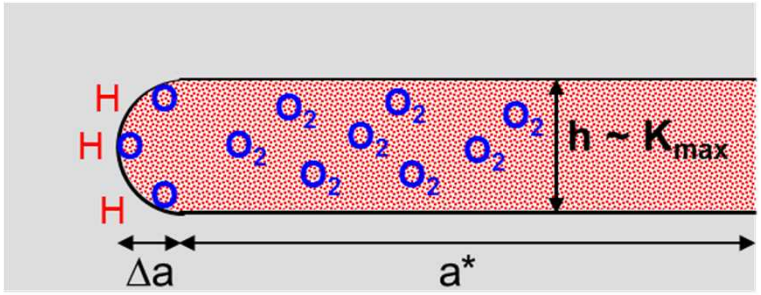


$$\Delta a_{crit} = \frac{0.3\chi D p_{tot}(1-\nu^2)}{f\pi S\theta_{crit}R_g TE\sigma_0}\left(\frac{\Delta K}{\sqrt{a^*}(1-R)}\right)^2$$

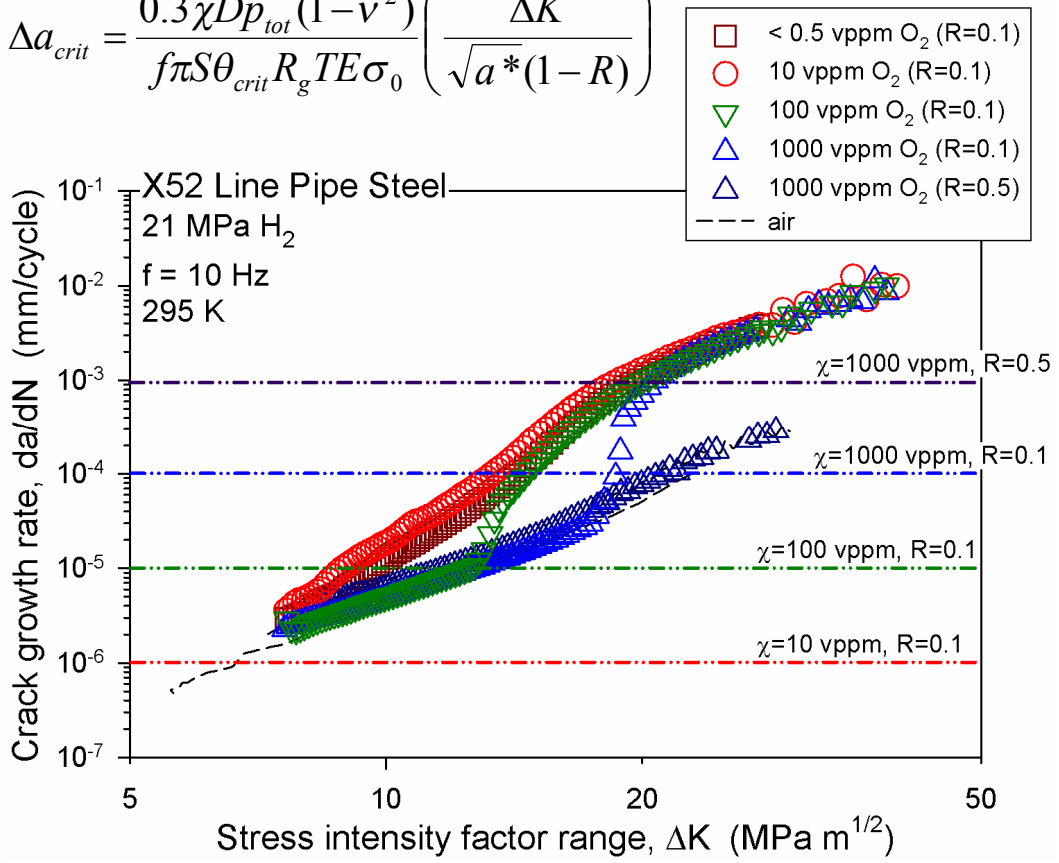


Sandia National Laboratories

# $H_2$-assisted cracking is multi-component phenomenon

## *Trends may be dominated by one component*

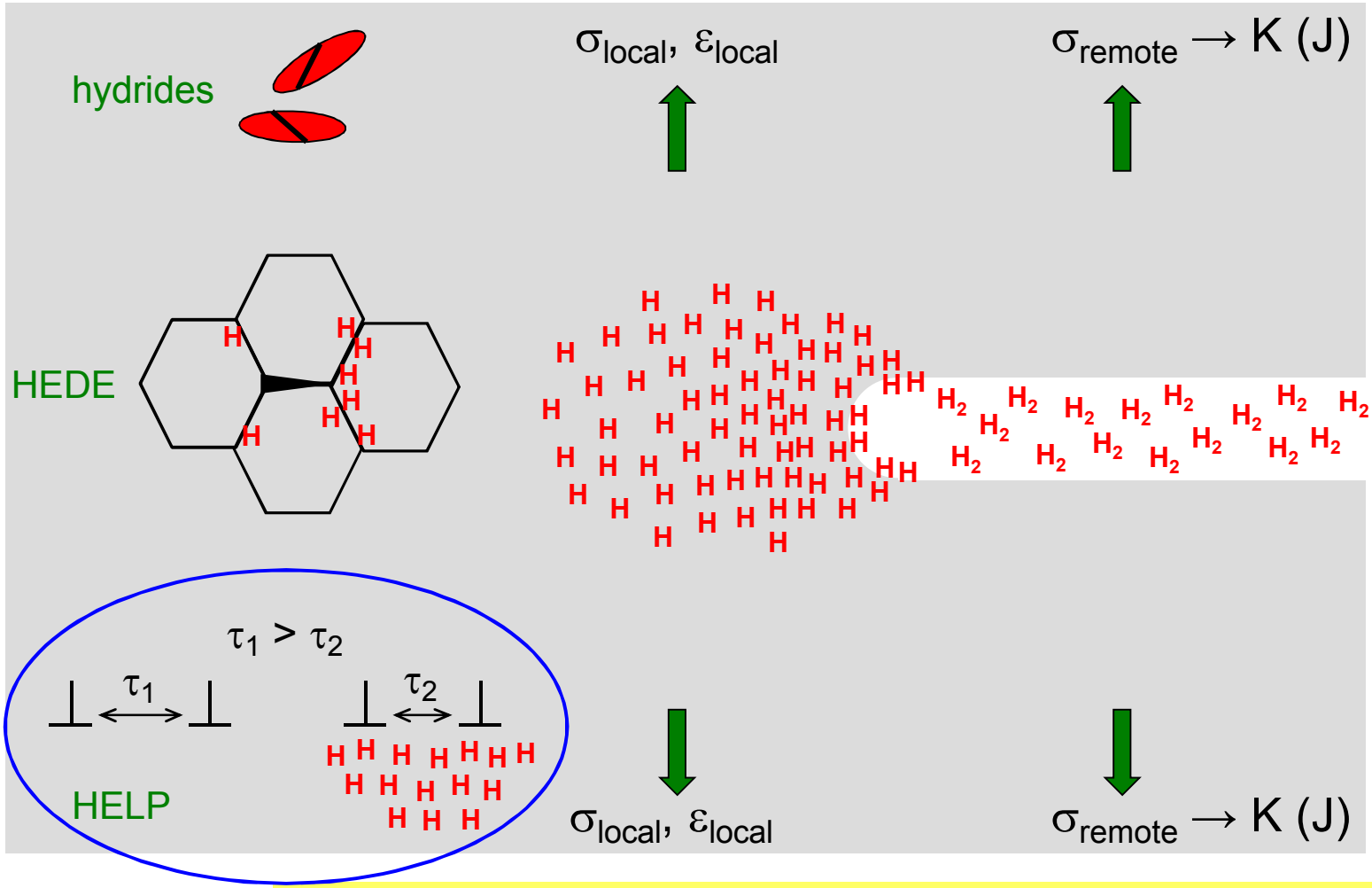


***Hydrogen-assisted cracking dictated by H-deformation interactions***

Sandia National Laboratories

# *Issue-driven research goal:* characterize H-assisted crack extension in stainless steel forgings

K.A. Nibur et al., *Acta Mater*, 2009

- 21Cr-6Ni-9Mn (21-6-9) alloy composition

| Cr | Ni | Mn | N | C | Si | P | S | FN |
|---|---|---|---|---|---|---|---|---|
| 21.0 | 6.7 | 8.9 | 0.23 | 0.030 | 0.35 | 0.020 | 0.00004 | <0.2 |

- Forged 927 °C + water quenched
  - Yield strength = 656 MPa
  - Ultimate tensile strength = 891 MPa

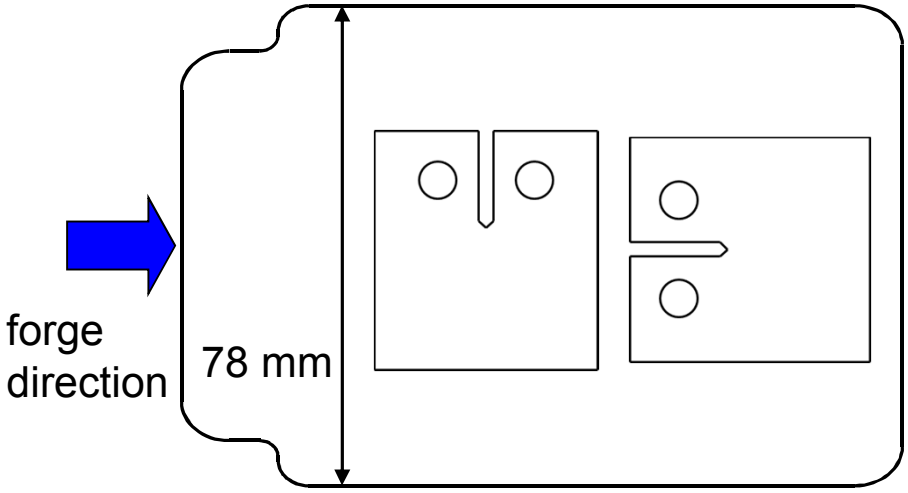


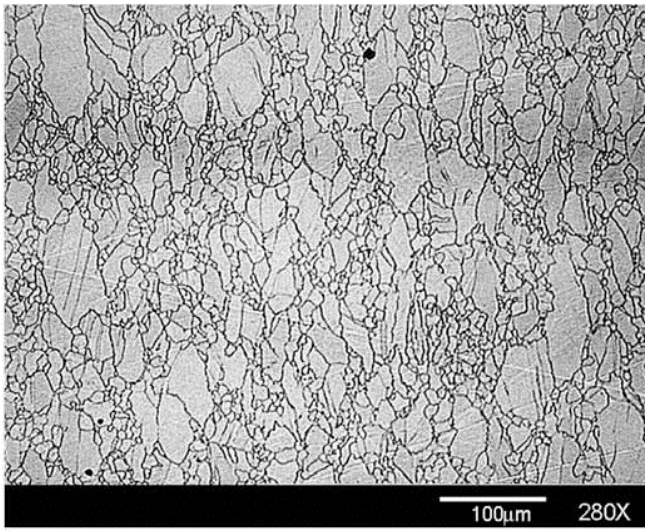


Sandia National Laboratories

# Measured crack growth resistance curves for H-charged 21-6-9 stainless steel

K.A. Nibur et al., *Acta Mater*, 2009

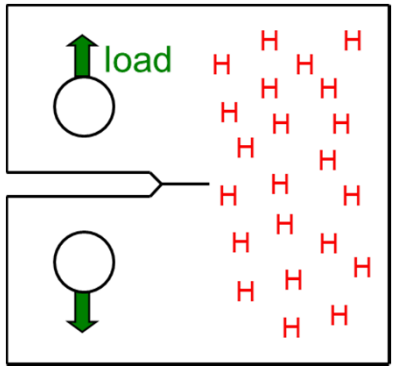


- Material
  - 21-6-9 austenitic stainless steel
- Environment
  - Thermal precharging in high-pressure $H_2$ (99.9999% $H_2$)
  - Pressure = 138 MPa $H_2$ (20,000 psi)
    Temperature = 300 °C
  - Resulting H concentration ~ 1.3 at%
- Mechanical loading
  - J vs. $\Delta a$ curves measured under rising displacement in air at 25 °C
  - Displacement rate = 0.4 mm/min

Sandia National Laboratories

# Hydrogen degrades crack growth resistance and alters fracture surface features

K.A. Nibur et al., *Acta Mater*, 2009

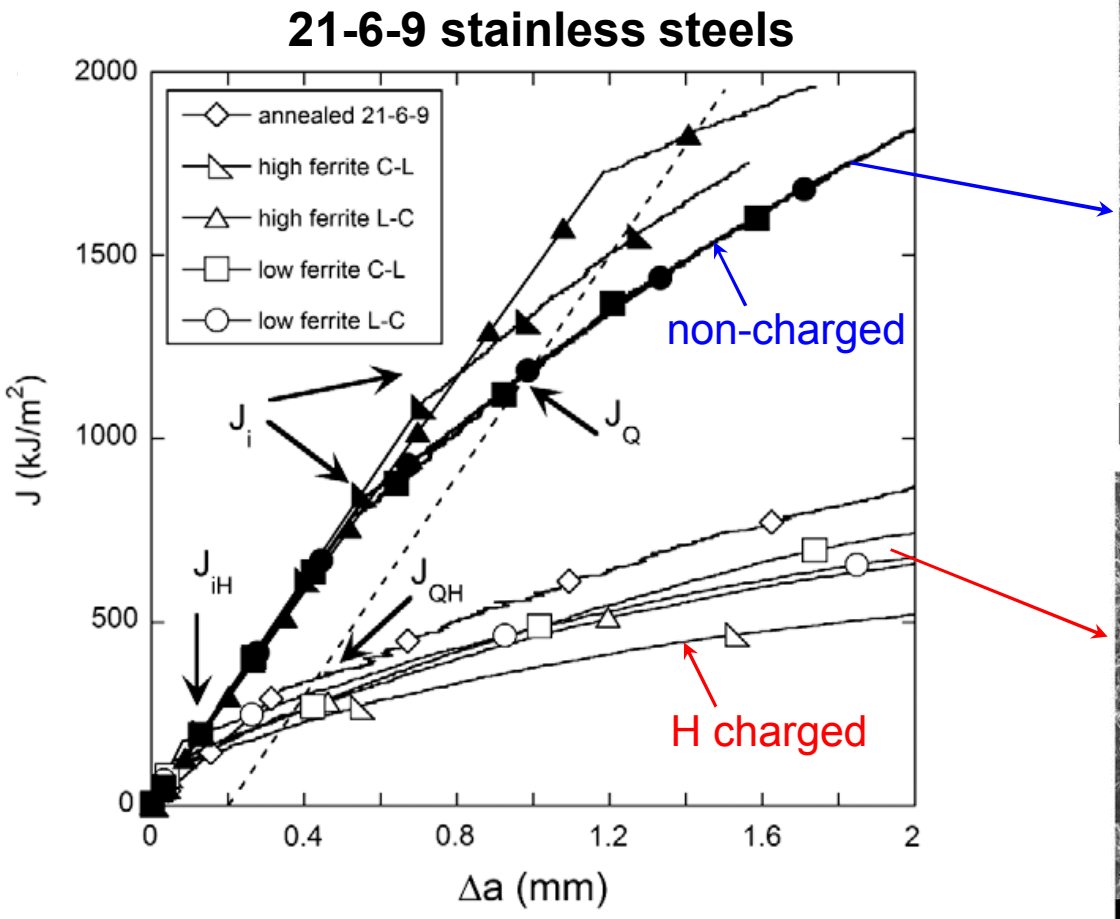


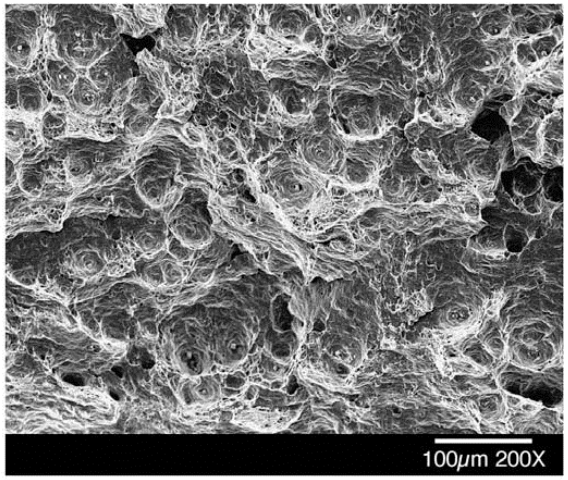


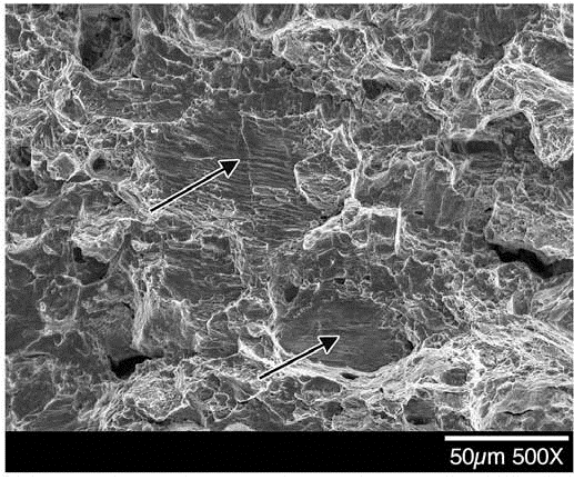


***What are H-material interactions and associated damage mechanisms that dictate observed trends?***

Sandia National Laboratories

# Indentation + AFM show that hydrogen amplifies height of deformation band intersections with surface

K.A. Nibur et al., *Acta Mater*, 2006

21-6-9

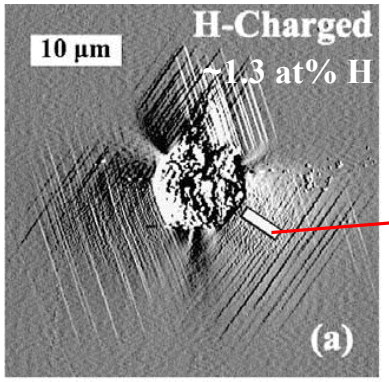


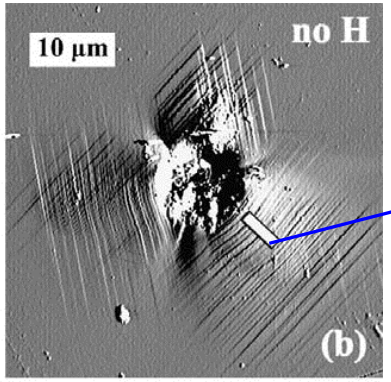


Atomic Force Microscopy (AFM) measurements

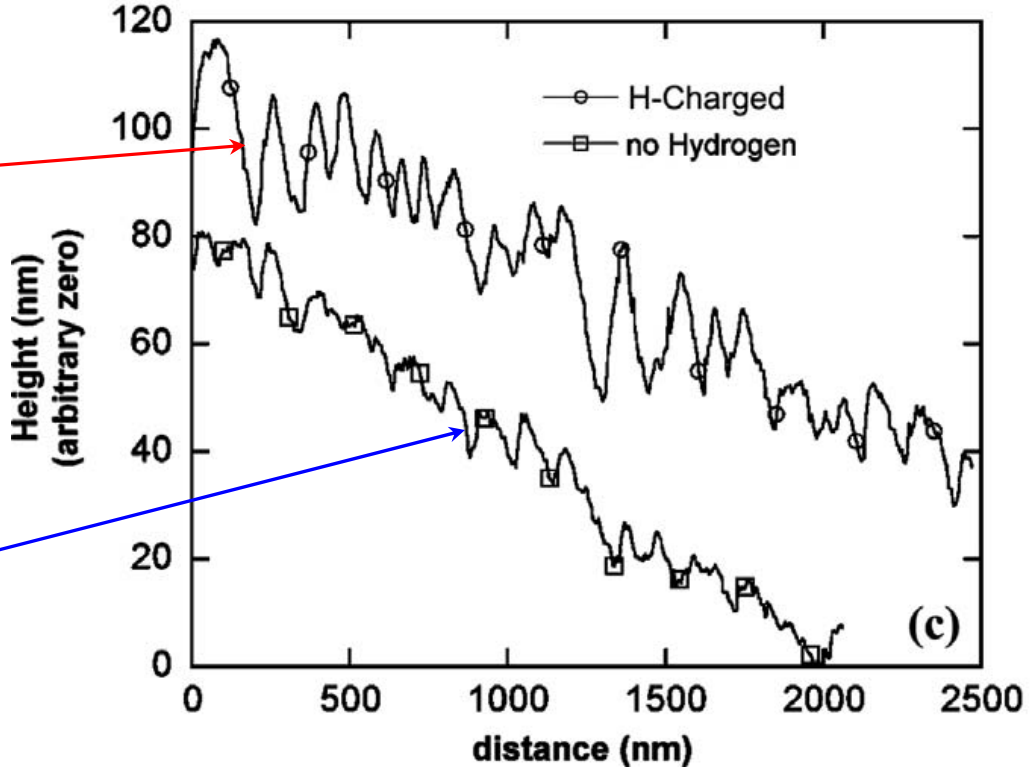


***Hydrogen promotes localized deformation in 21-6-9 stainless steel***

Sandia National Laboratories

# H-induced localized deformation leads to void damage at band intersections

K.A. Nibur et al., *Acta Mater*, 2009

Fracture profile from H-charged 21-6-9

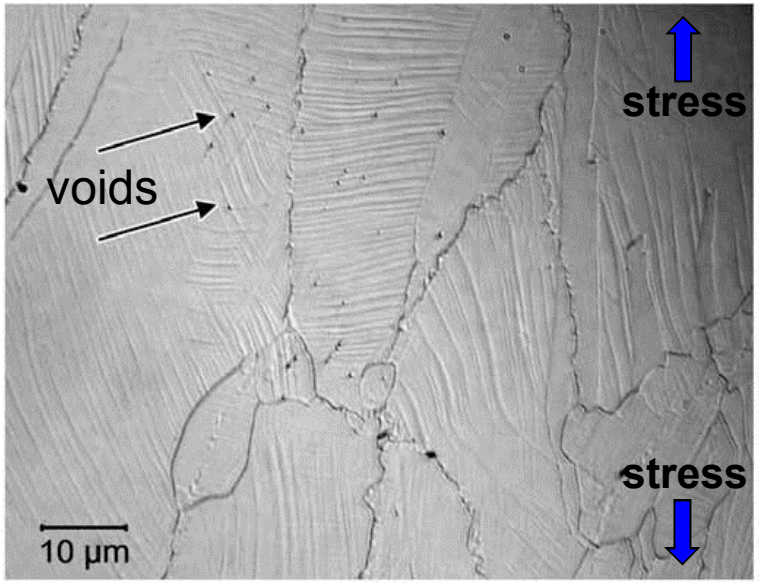


optical image

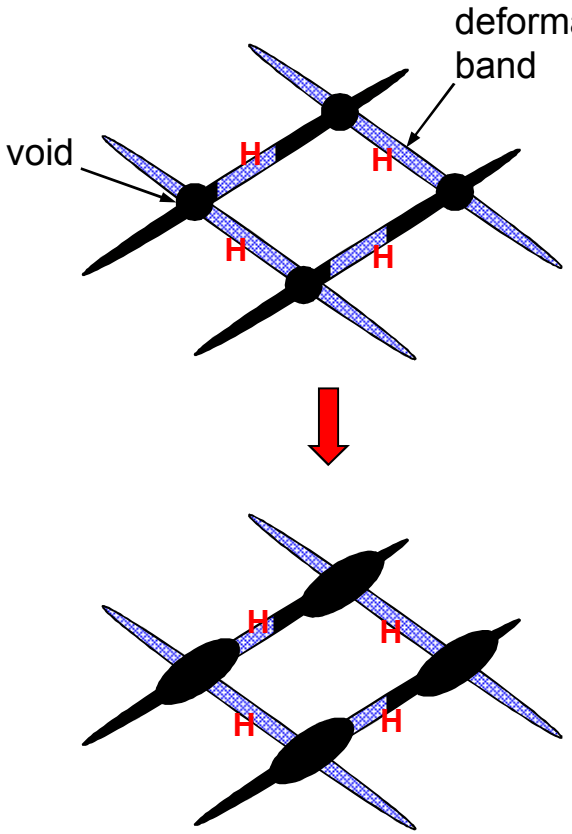


***Observations provide concrete link between H-affected deformation and material damage in bulk specimens***

Sandia National Laboratories

# Results from other systems demonstrate that localized deformation alone can govern damage

Ti-11 at% Mo (no H)

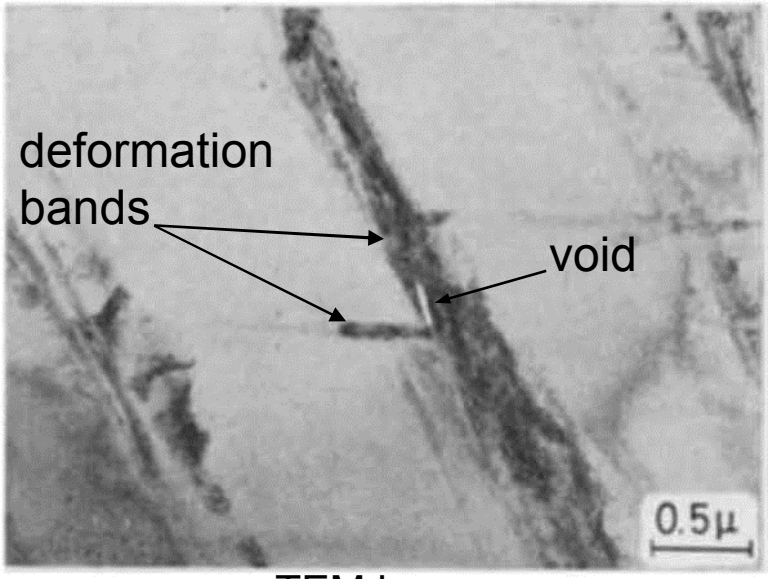


TEM image

A. Gysler et al., *Acta Metall*, 1974

21-6-9 (H-charged)

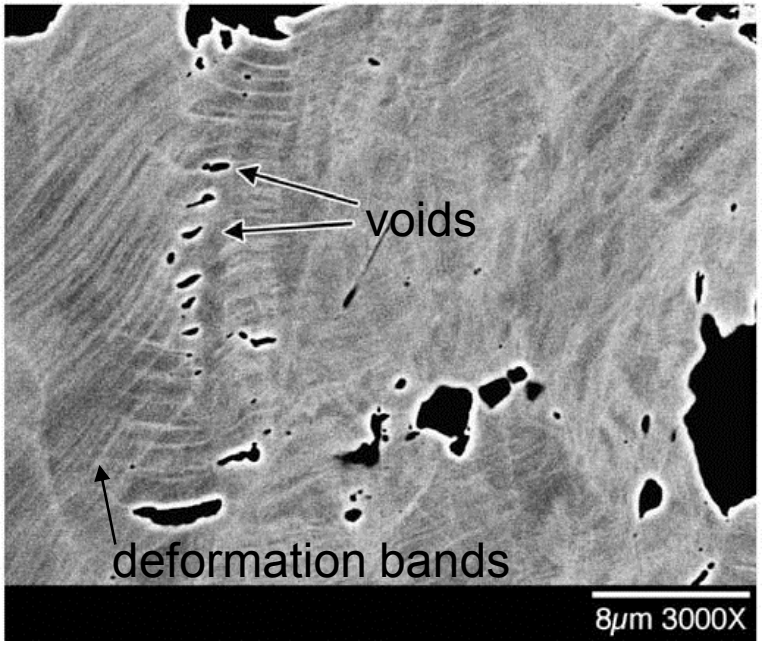


BEI image

K.A. Nibur et al., *Acta Mater*, 2009

- ***Can H-assisted damage in 21-6-9 be attributed solely to H-induced localized deformation?***
- ***Does hydrogen directly lower fracture resistance?***

Sandia National Laboratories

# Gaseous Hydrogen-Assisted Cracking: A Comprehensive View

- $H_2$-assisted cracking most effectively analyzed by recognizing its multiple components → *inherently multi-disciplinary*
  - Crack-tip strain fields driving hydrogen-induced damage *(solid mechanics)*
  - Gas-surface interactions governing crack-tip hydrogen uptake *(surface science)*
  - Hydrogen-material interactions leading to damage *(materials science)*

- Conclusions from three research stories:
  - Strain-controlled fracture criterion coupled with strain field amplitude explains difference between $H_2$-assisted cracking thresholds
  - Model based on diffusion-limited oxygen adsorption quantifies effect of mechanical and environmental variables on $H_2$-accelerated cracking
  - H-affected deformation may have direct link to material damage in bulk specimens

# Acknowledgments


- Sandia National Laboratories
  - Kevin Nibur (currently at Hy-Performance Materials Testing)
  - Chris San Marchi
  - Dorian Balch
  - Jay Foulk
  - Joe Ronevich
  - Zach Harris
  - Ken Lee
  - Jeff Campbell
  - Mark Zimmerman
- International Institute for Carbon Neutral Energy Research
  - Prof. Petros Sofronis (University of Illinois)
  - Prof. Reiner Kirchheim (University of Göttingen)
  - Prof. Alex Staykov (Kyushu University)
  - Dr. Mohsen Dadfarnia (University of Illinois)


Sandia National Laboratories

# Back-up Slides

# SNL core capability in hydrogen embrittlement features Hydrogen Effects on Materials Lab

- Static-loading crack-growth system
  - Wedge opening load (WOL) and double cantilever beam (DCB) specimens
  - $H_2$ pressure up to 200 MPa
  - Temperature -70 to 170 $^oC$
- Dynamic-loading crack-growth system
  - Compact tension (CT) and single edge notch (SEN) specimens
  - $H_2$ pressure up to 138 MPa
  - New pressure vessel design with target temperatures -100 to 200 $^oC$

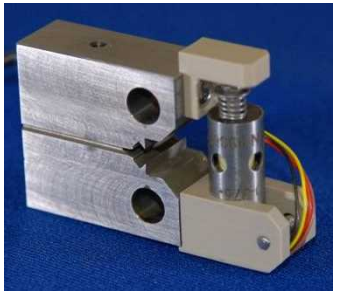

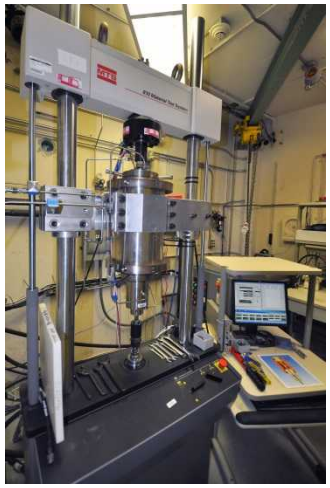

***Materials testing in $H_2$ supports technology development in several mission areas***

Sandia National Laboratories

# Grain-boundary structure affects susceptibility to H-induced intergranular cracking

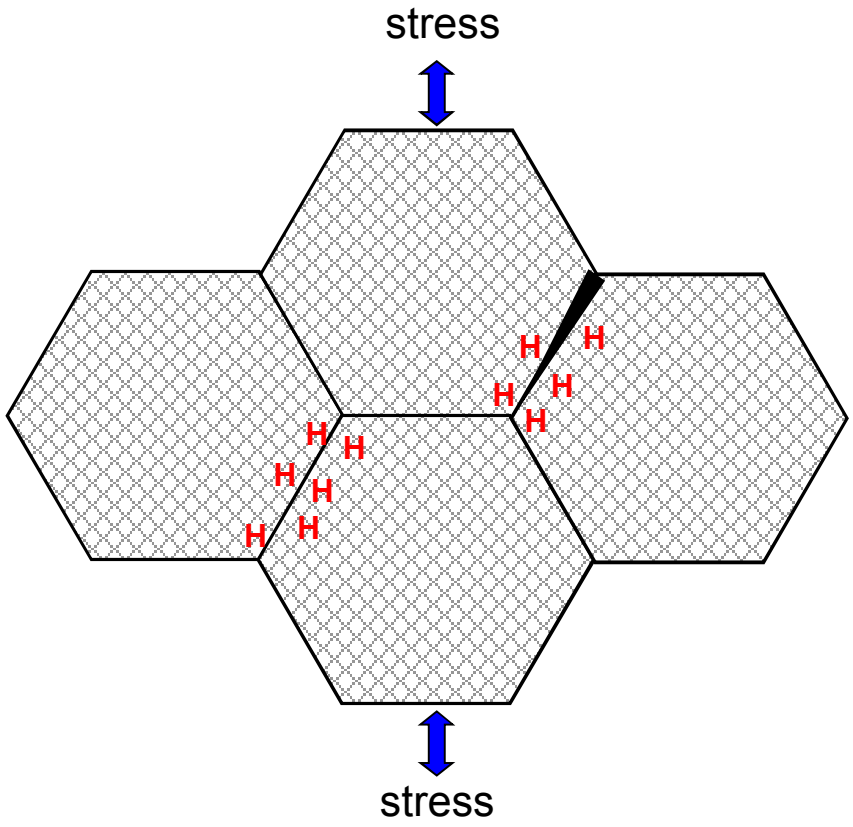


S. Bechtle,, et al., *Acta Mater,* 2009

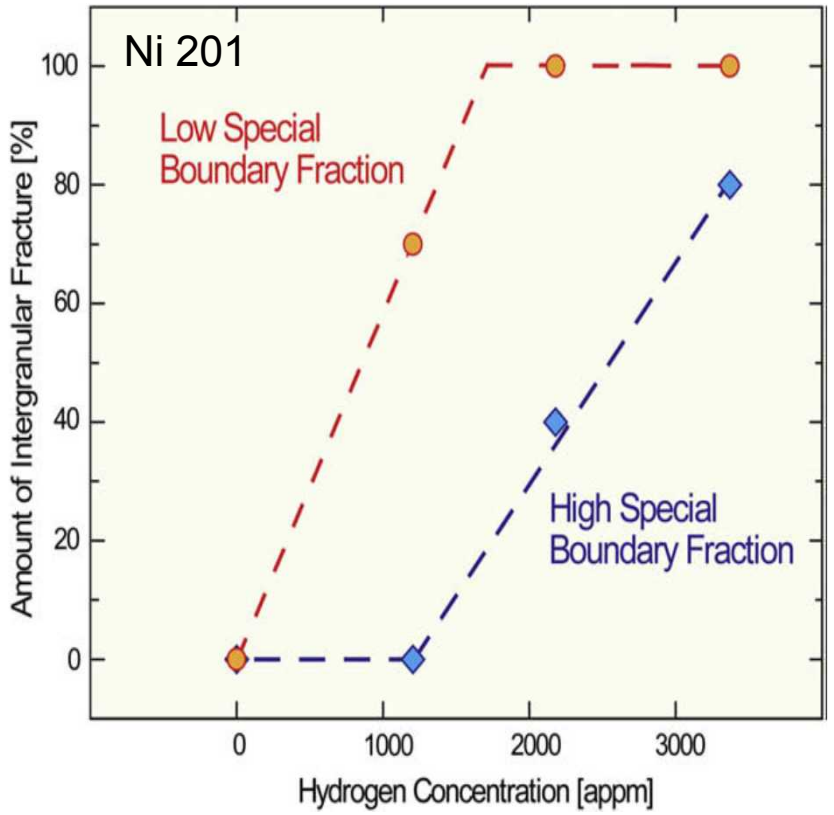


- Special (i.e., CSL) boundaries less susceptible to H-induced cracking than random boundaries

Sandia National Laboratories

# Hydrogen-enhanced localized plasticity (HELP) conclusively demonstrated for numerous metals

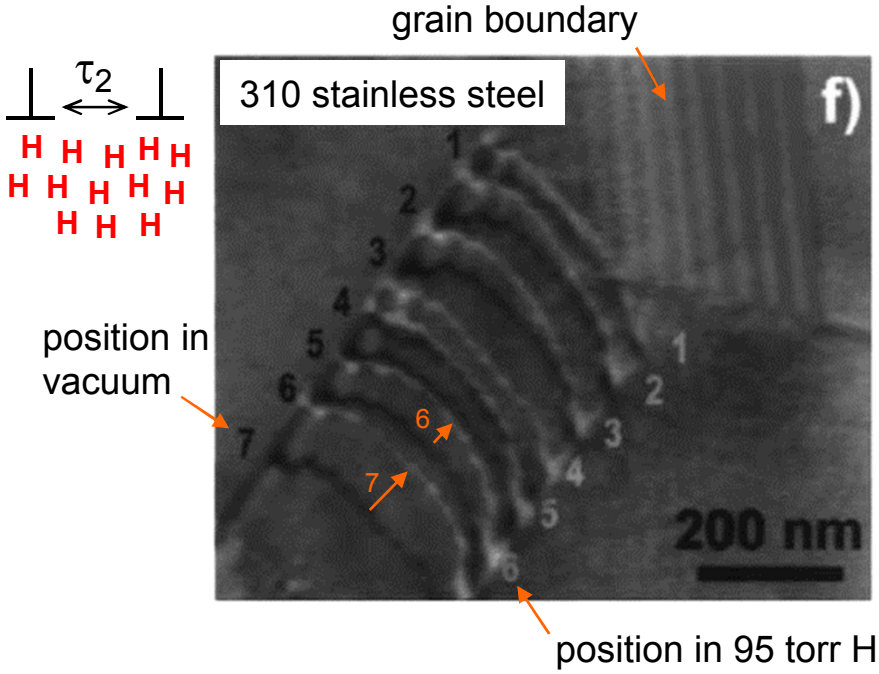


I. Robertson, *Eng Fract Mech*, 2001

- Enhanced dislocation mobility (softening) and stress shielding concept demonstrated through *in situ* TEM experiments
- Other observations:
  - H stabilizes edge component of mixed dislocations
  - H promotes localized deformation

***Unresolved issue:*** "What is the detailed mechanism by which the enhanced dislocation mobility causes fracture in *bulk* specimens?" H. Birnbaum, *CDI 96*, 1997

# Yield strength and alloy composition of martensitic pressure vessel steels

**Table I. Yield Strength and Composition of the Pressure Vessel Steels**

| Alloy | Yield Strength (MPa) | C | Cr | Cu | Mo | Ni | Al | Mn | Si | P | S | Fe |
|---|---|---|---|---|---|---|---|---|---|---|---|---|
| 4130X | 607 | 0.29 | 0.92 | nr | 0.19 | nr | 0.035 | 0.62 | 0.28 | 0.008 | 0.004 | bal |
| 4130X | 641 | 0.30 | 0.95 | nr | 0.18 | nr | 0.030 | 0.63 | 0.28 | 0.008 | 0.005 | bal |
| SA372 grade *J* | 641 | 0.46 | 0.94 | nr | 0.18 | nr | nr | 0.92 | 0.25 | 0.011 | 0.006 | bal |
| SA372 grade *J* | 717 | 0.48 | 0.96 | nr | 0.18 | nr | 0.026 | 0.92 | 0.30 | 0.010 | 0.002 | bal |
| SA372 grade *J* | 730 | 0.48 | 1.01 | nr | 0.19 | nr | nr | 0.98 | 0.27 | 0.013 | 0.005 | bal |
| SA372 grade *J* | 736 | 0.47 | 0.96 | nr | 0.19 | nr | 0.032 | 0.92 | 0.30 | 0.012 | 0.003 | bal |
| SA372 grade *J* | 783 | 0.49 | 0.99 | nr | 0.18 | nr | nr | 0.93 | 0.28 | 0.008 | 0.004 | bal |
| SA372 grade *L* | 731 | 0.4 | 0.82 | 0.1 | 0.26 | 1.93 | 0.022 | 0.75 | 0.28 | 0.006 | 0.007 | bal |
| SA372 grade *L* | 1053 | 0.4 | 0.82 | 0.1 | 0.26 | 1.93 | 0.022 | 0.75 | 0.28 | 0.006 | 0.007 | bal |
| DOT-3T | 900 *A* | 0.45 | 0.97 | nr | 0.18 | nr | 0.034 | 0.86 | 0.25 | 0.013 | 0.006 | bal |
| DOT-3T | 900 *B* | 0.44 | 0.99 | nr | 0.18 | nr | 0.031 | 0.85 | 0.26 | 0.007 | 0.003 | bal |

nr = not reported.

# $K_{THi}$ reaches lower bound as loading rate decreases

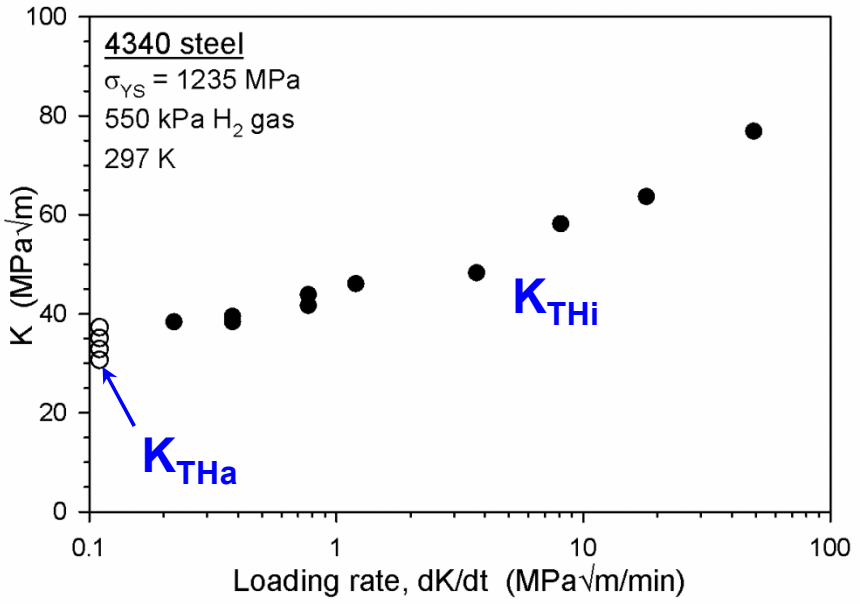


Clark and Landes, *ASTM STP 610*, 1976

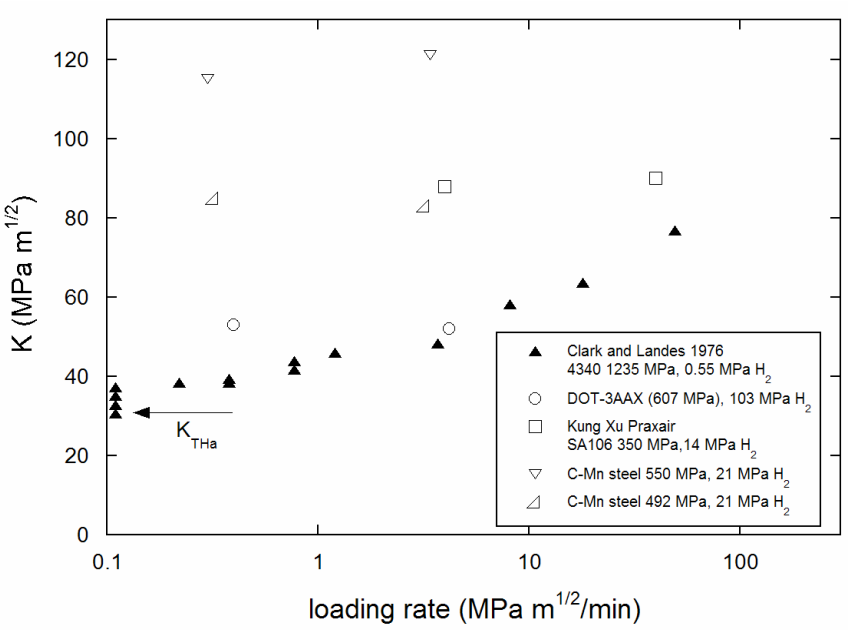


K.A. Nibur et al., SAND2010-4633, 2010

Sandia National Laboratories

# Higher $K_{THa}$ compared to $K_{THi}$ not attributed to crack arrest near back face in conventional WOL

Conventional WOL specimen

Chevron-notched WOL specimen

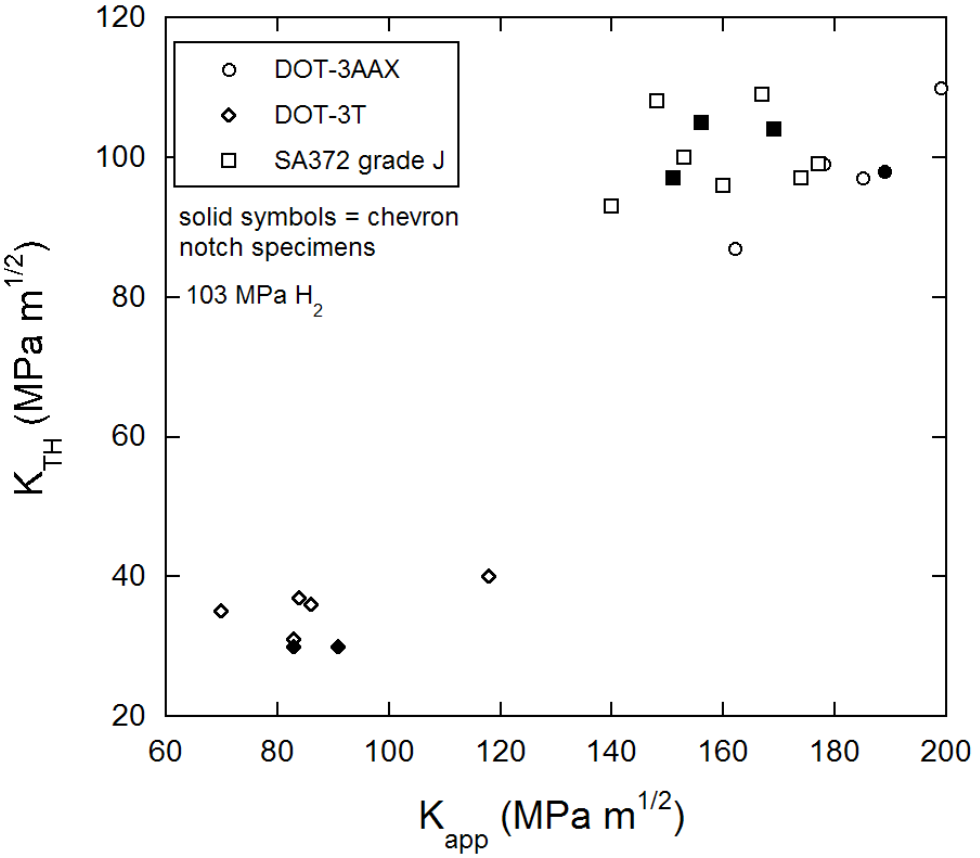


- Chevron-notched WOL specimen
  - Reduced compliance leads to lower initial loads
  - Lower initial loads allow shorter precracks, which limit final crack length at $K_{THa}$

Sandia National Laboratories

# Plasticity-related hydrogen-induced cracking assumed for martensitic pressure vessel steels

4130X
100 MPa $H_2$ gas

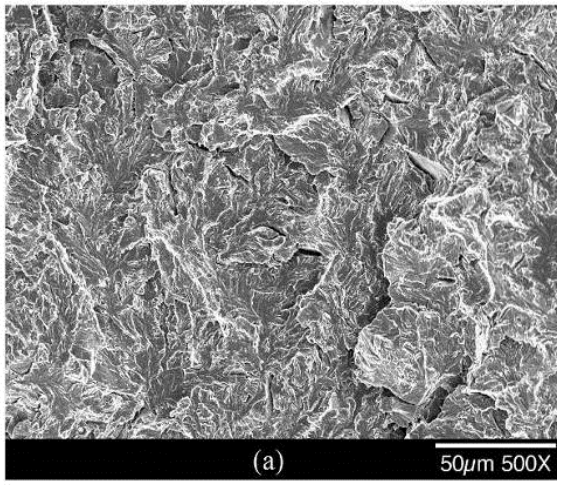


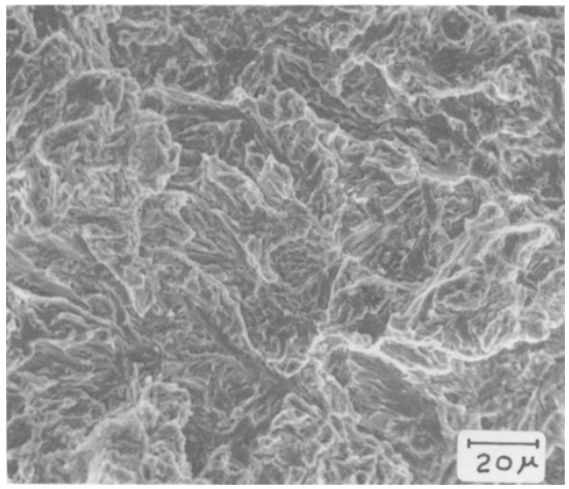


HY 130-type
0.2 MPa $H_2$ gas

Takeda and McMahon, *Metall Trans A*, 1981

slip lines at notch root

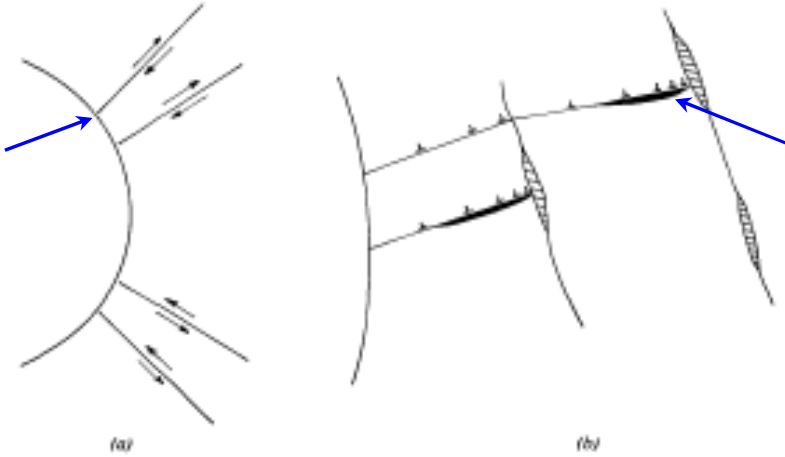

plasticity-related hydrogen-induced cracking (PRHIC): glide plane decohesion

Sandia National Laboratories

# Elastic unloading behind crack tip leads to distinct strain field for propagating crack vs. stationary crack

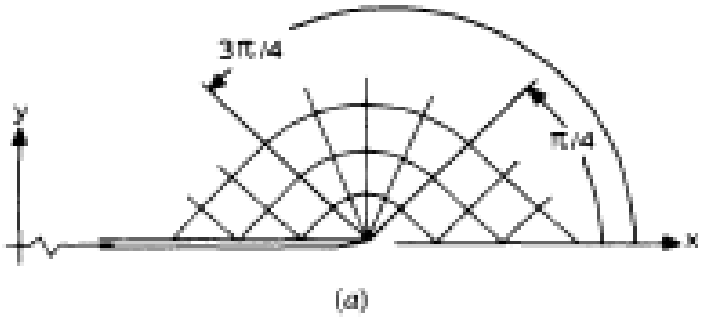


stationary crack

unloading

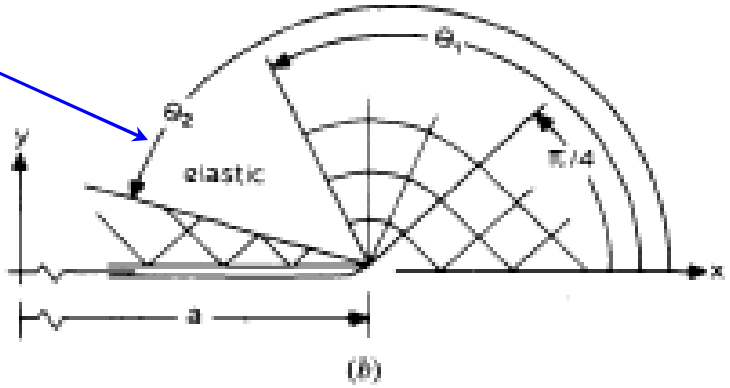


propagating crack

Plane strain slip-line representation of crack tip stress states of Prandtl field for stationary crack and propagating crack

Ritchie and Thompson, *Metall Trans A*, 1985

Sandia National Laboratories

# Stress fields near crack tip similar for stationary and propagating cracks

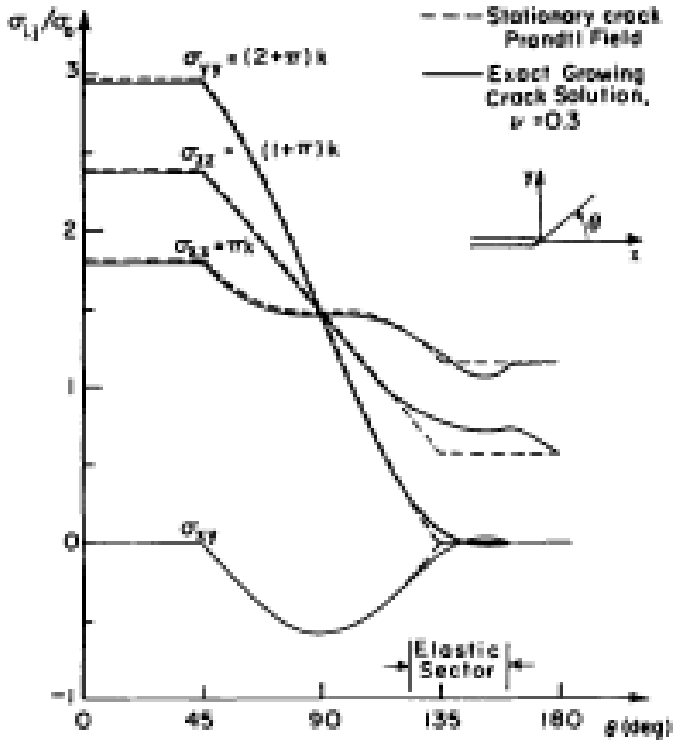


Local stresses ahead of crack tip as a function of angle θ for stationary crack and propagating crack

Ritchie and Thompson, *Metall Trans A*, 1985

Sandia National Laboratories

# FEM simulations of plastic strain ahead of propagating and stationary cracks

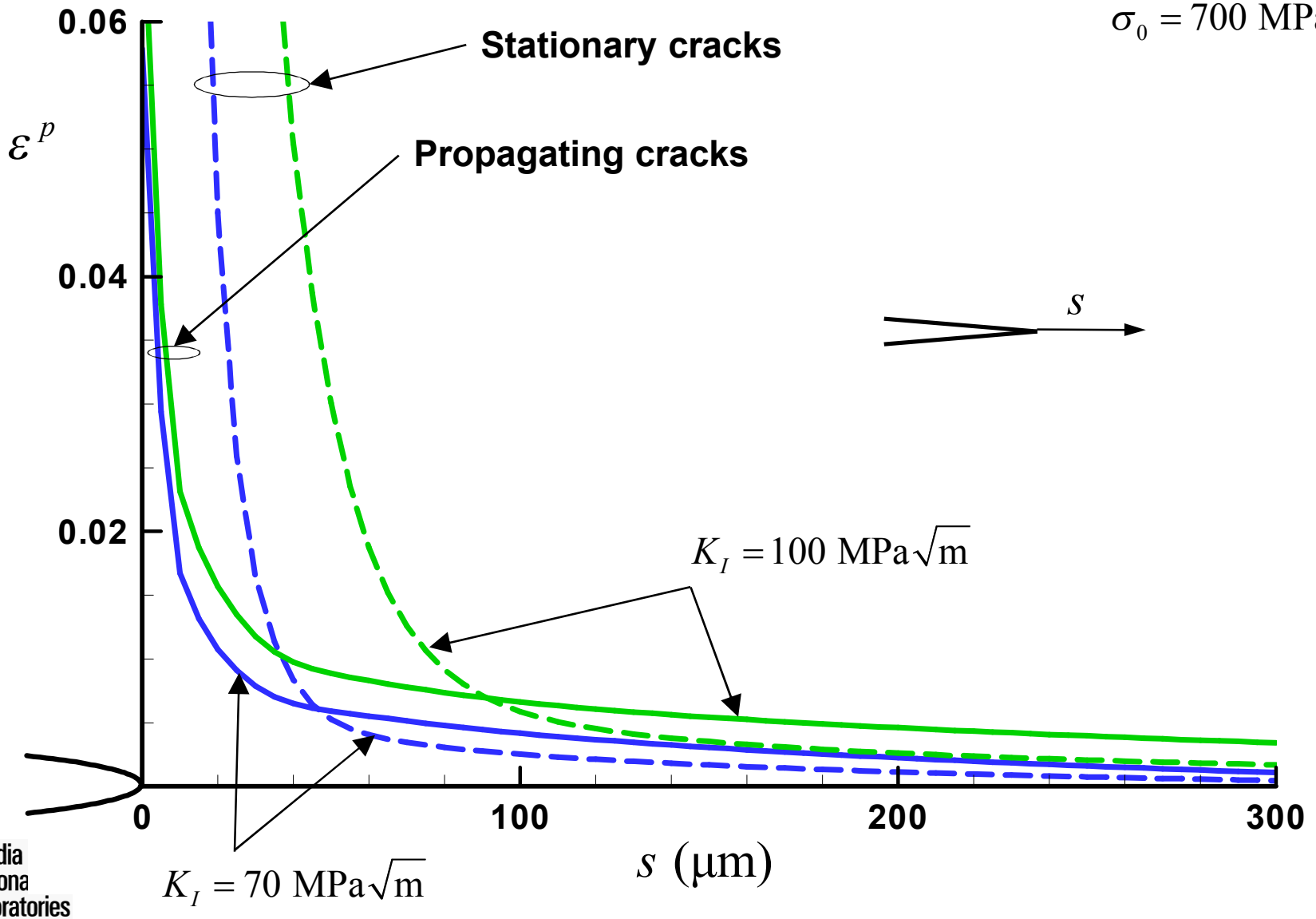


Sandia National Laboratories

# FEM simulations of opening stress ahead of propagating and stationary cracks

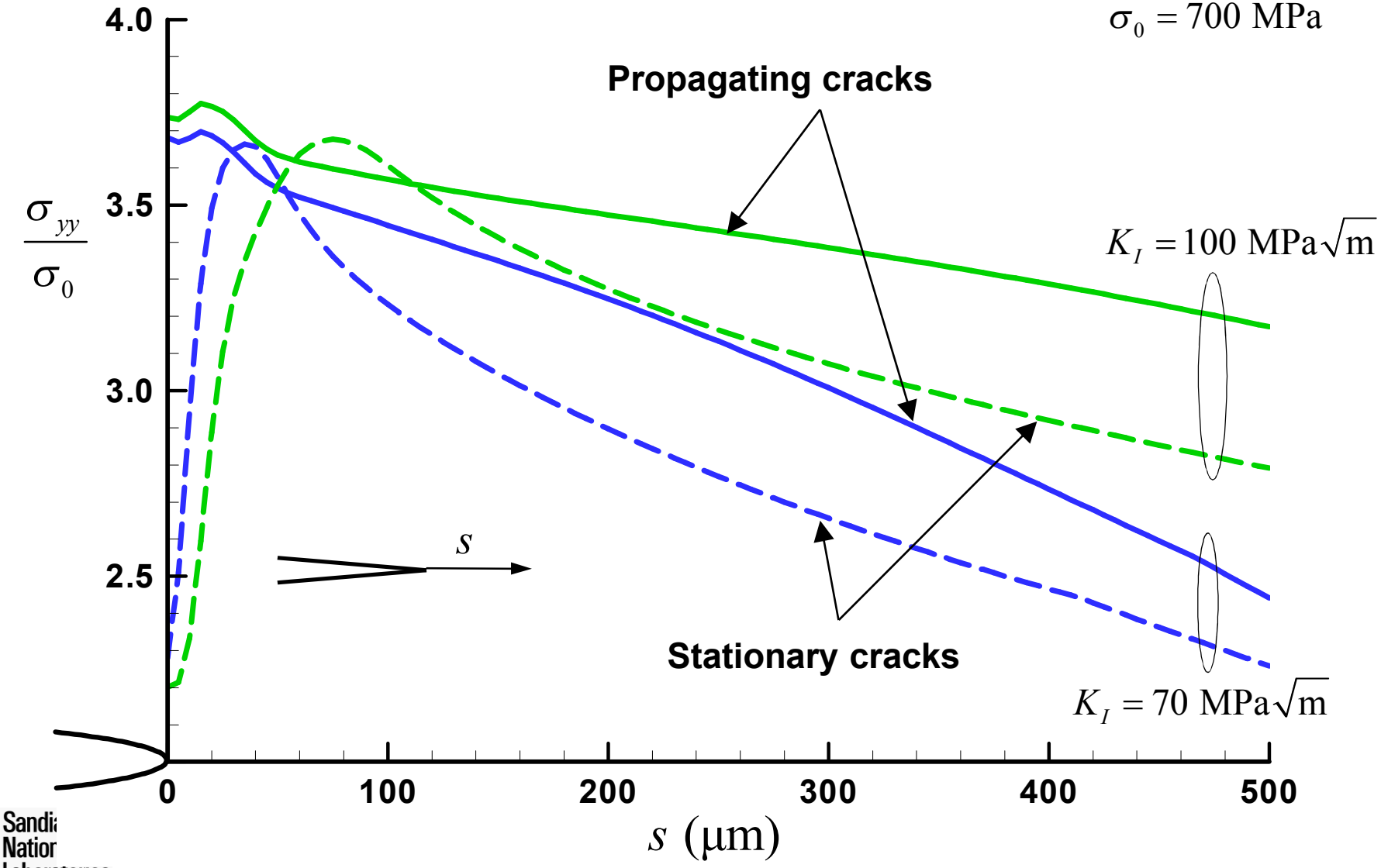


Sandia National Laboratories

# Gas constituents such as $O_2$ can inhibit $H_2$-accelerated fatigue cracking in steels

H. Johnson, *Stress Corrosion Cracking and Hydrogen Embrittlement of Iron Based Alloys*, 1977

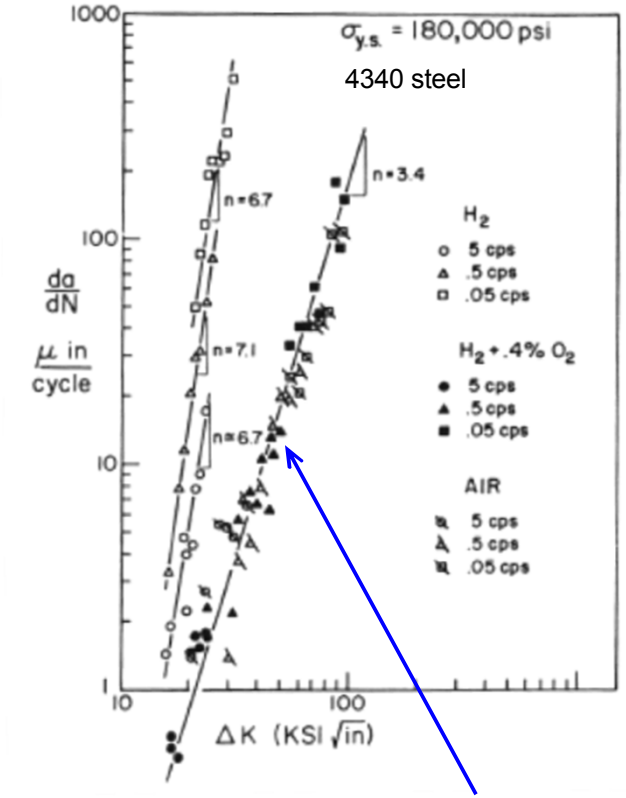


R. Wei and R. Gangloff, *ASTM STP 1020*, 1989

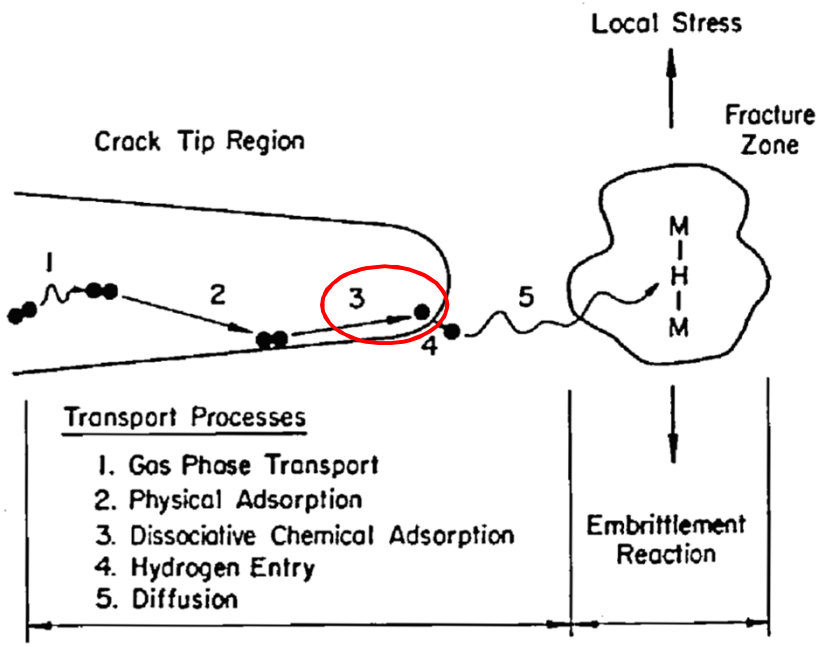


*How is $O_2$ inhibition affected by variables such as $\Delta K$, frequency, R ratio, and $O_2$ content?*

Sandia National Laboratories

# Density functional theory (DFT) simulations suggest mechanism for $O_2$ inhibition of H uptake

Potential energy surface scan for $H_2$ approaching Fe(100) surface

$H_2$ molecule approaches directly on top Fe atom

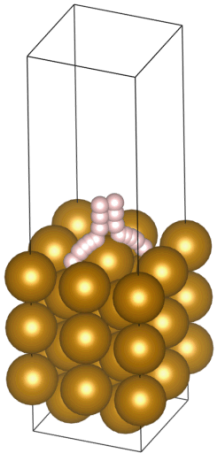

Potential energy surface scan for $H_2$ approaching Fe(100) surface with preadsorbed O atoms

$H_2$ molecule approaches directly on top Fe atom

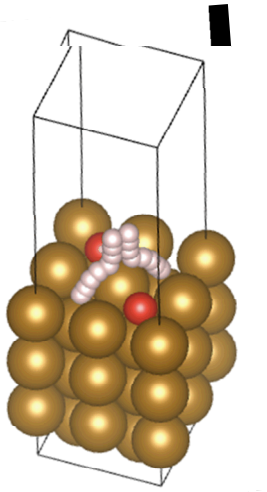

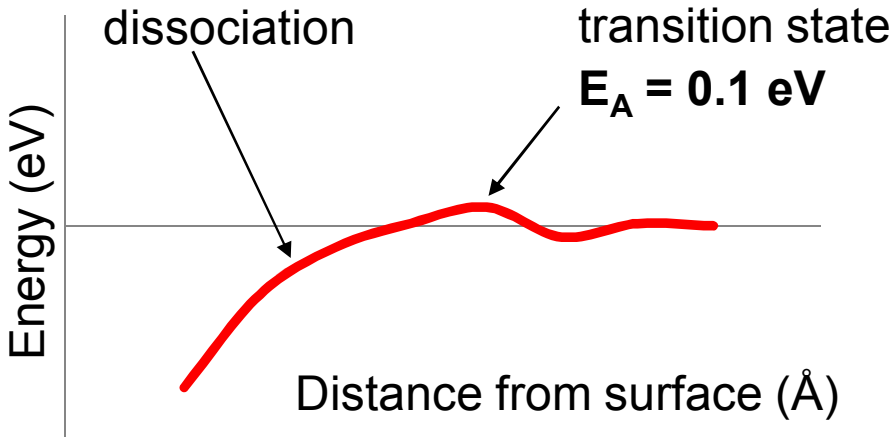


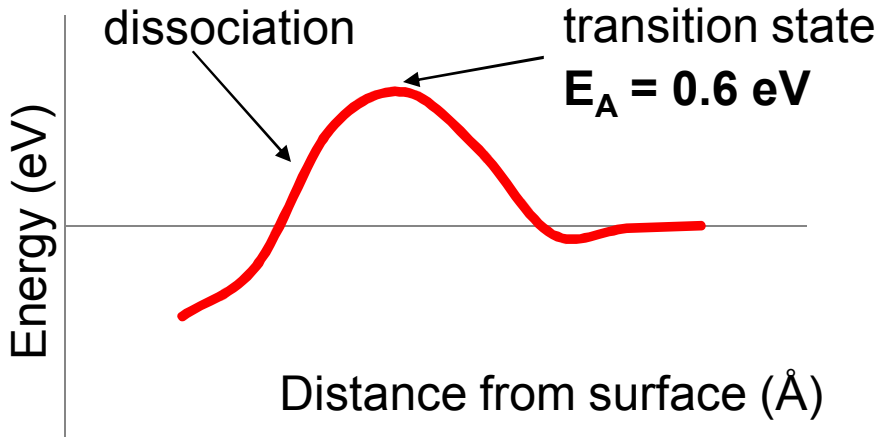


Staykov et al., *Int J Quantum Chemistry*, 2014

***Preadsorbed oxygen on iron surface raises activation energy for $H_2$ dissociation***

Sandia National Laboratories

# Electron density difference method provides insight into dissociation inhibition mechanism

$H_2$ approaching Fe(100) surface

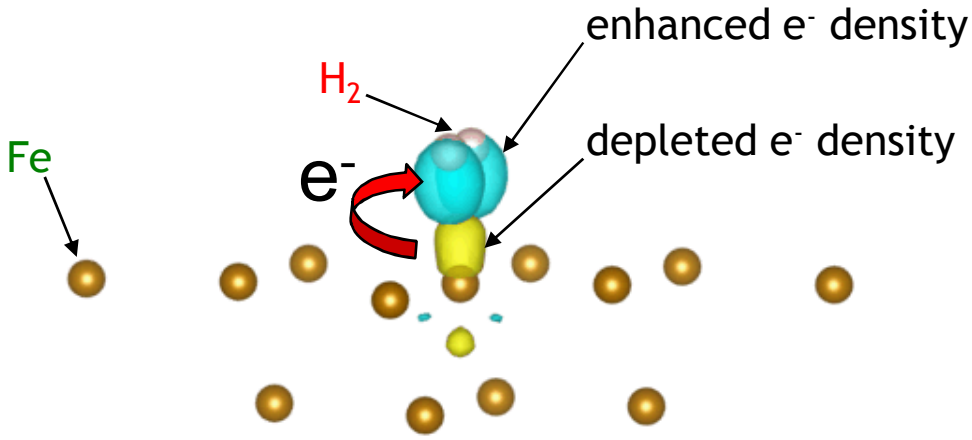


$H_2$ approaching Fe(100) surface with preadsorbed O atoms

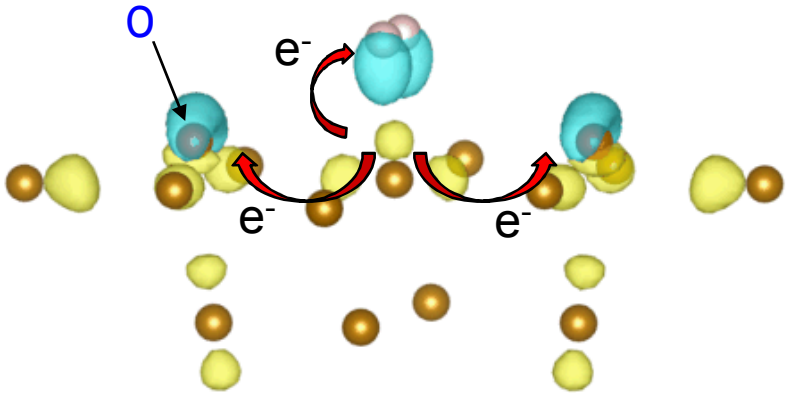


- *Oxygen atoms on surface localize $e^-$ density, reducing ability of neighboring Fe atoms to donate $e^-$ to $H_2$*
- ***Less $e^-$ density available for $H_2$ activation: dissociation hindered***

Sandia National Laboratories

# DFT simulations provide rationale for preferential adsorption of $O_2$ in mixed $H_2$+$O_2$ gas

Potential energy surface scan for $H_2$ approaching Fe(100) surface

- $H_2$ is detected at 2.6 Å
- Weak attractive force
- Activation barrier: not all $H_2$ molecules dissociate

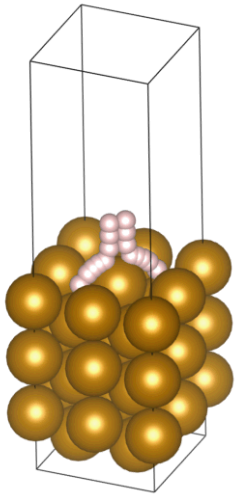

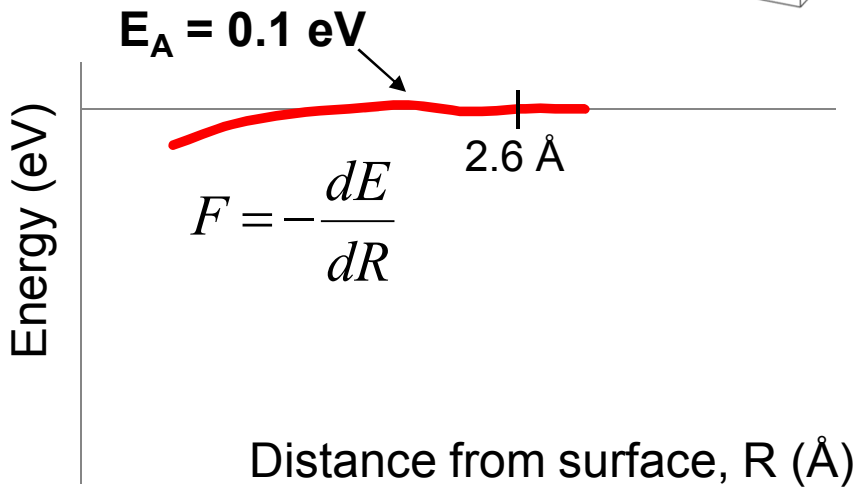


Potential energy surface scan for $O_2$ approaching Fe(100) surface

- $O_2$ is detected at 3.6 Å
- Strong attractive force
- No activation barrier: all $O_2$ molecules dissociate

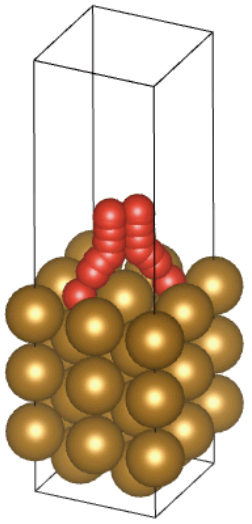

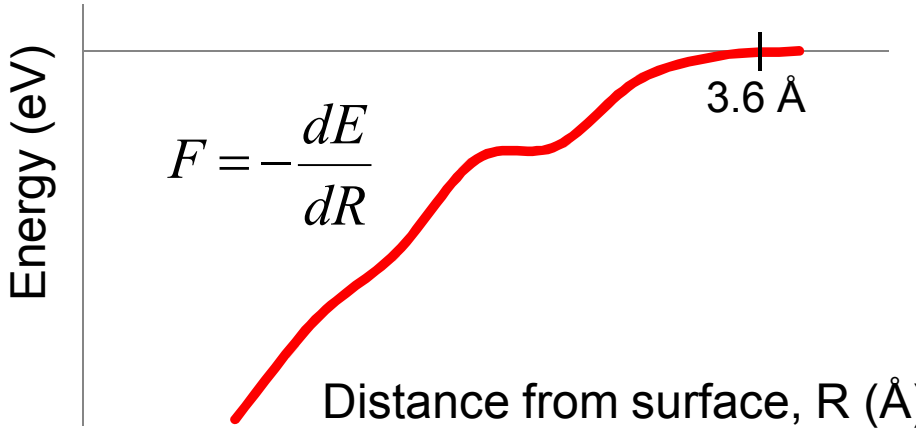


***Strong attractive force and absence of activation barrier allow $O_2$ to out-compete $H_2$***

Sandia National Laboratories

# DFT simulations define potential scenario for $O_2$ inhibition of H uptake

**Key elements in $O_2$ inhibition scenario:**

- *$O_2$ detected deeper in gas volume compared to $H_2$*
- *Force on $O_2$ >> force on $H_2$*
  - ***$O_2$ can out-compete $H_2$ for adsorption sites***
- ***Adsorbed O leads to repulsive force on $H_2$***

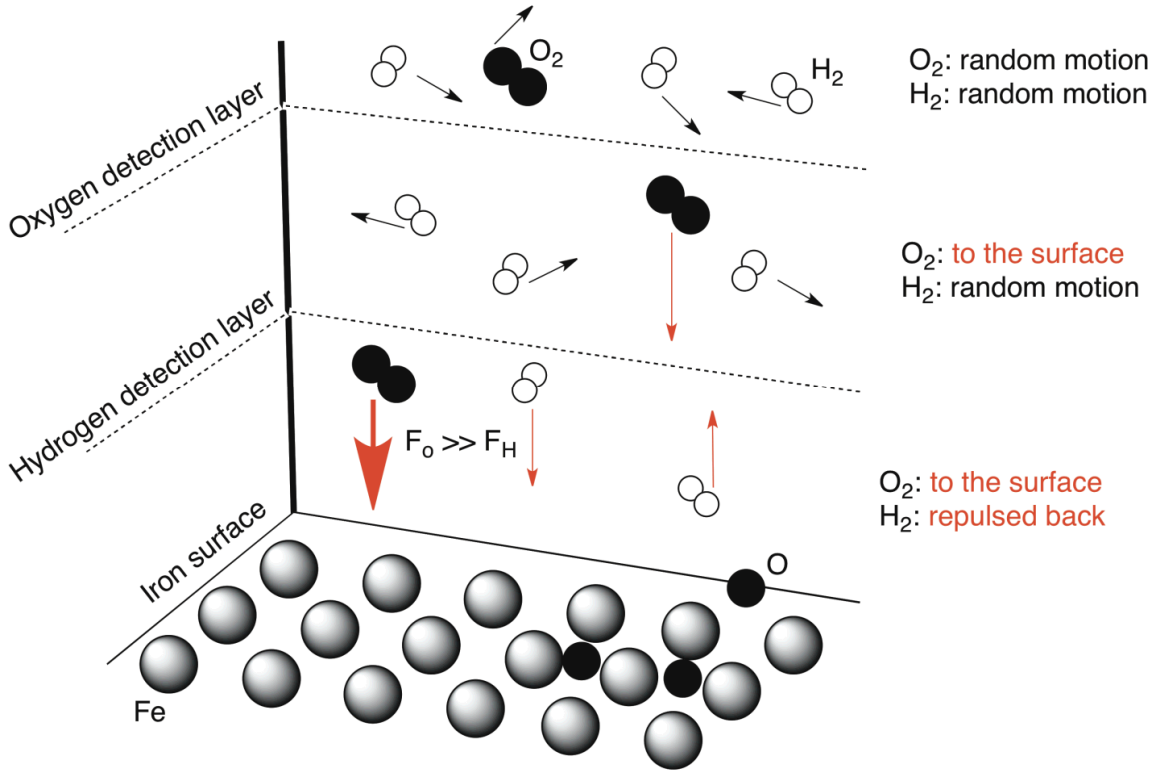


Sandia National Laboratories

# Density Functional Theory (DFT): Methods of Calculation

**Theory: plane wave DFT**

Program: VASP
Functional: optB86b-vdW
(includes long-range interactions)
Results verified with GGA-PBE

Spin polarized calculations
(accurate spin guess applied)

Energy cut-off: 400 eV
K-points: 8x8x8 bulk; 3x3x1 surface

Transition state search:
climbing nudged elastic band method
8 images per band

Analysis:
Bader population analysis
Electron density difference method

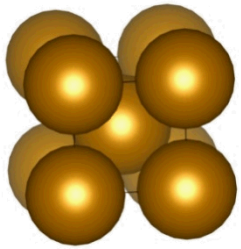

**BCC Fe lattice**
Ferromagnetic coupling

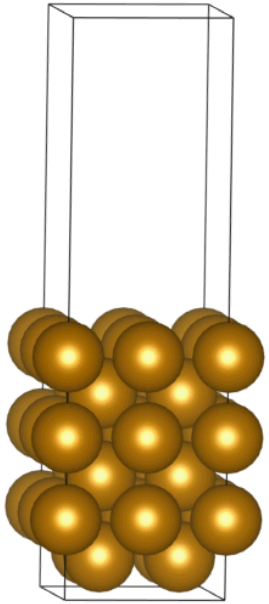

**2x2 surface supercell**
6 layers Fe atoms
12 A Vacuum slab

Top 3 layers are relaxed
Bottom 3 layers are fixed

# $H_2$ starting geometries on Fe surface

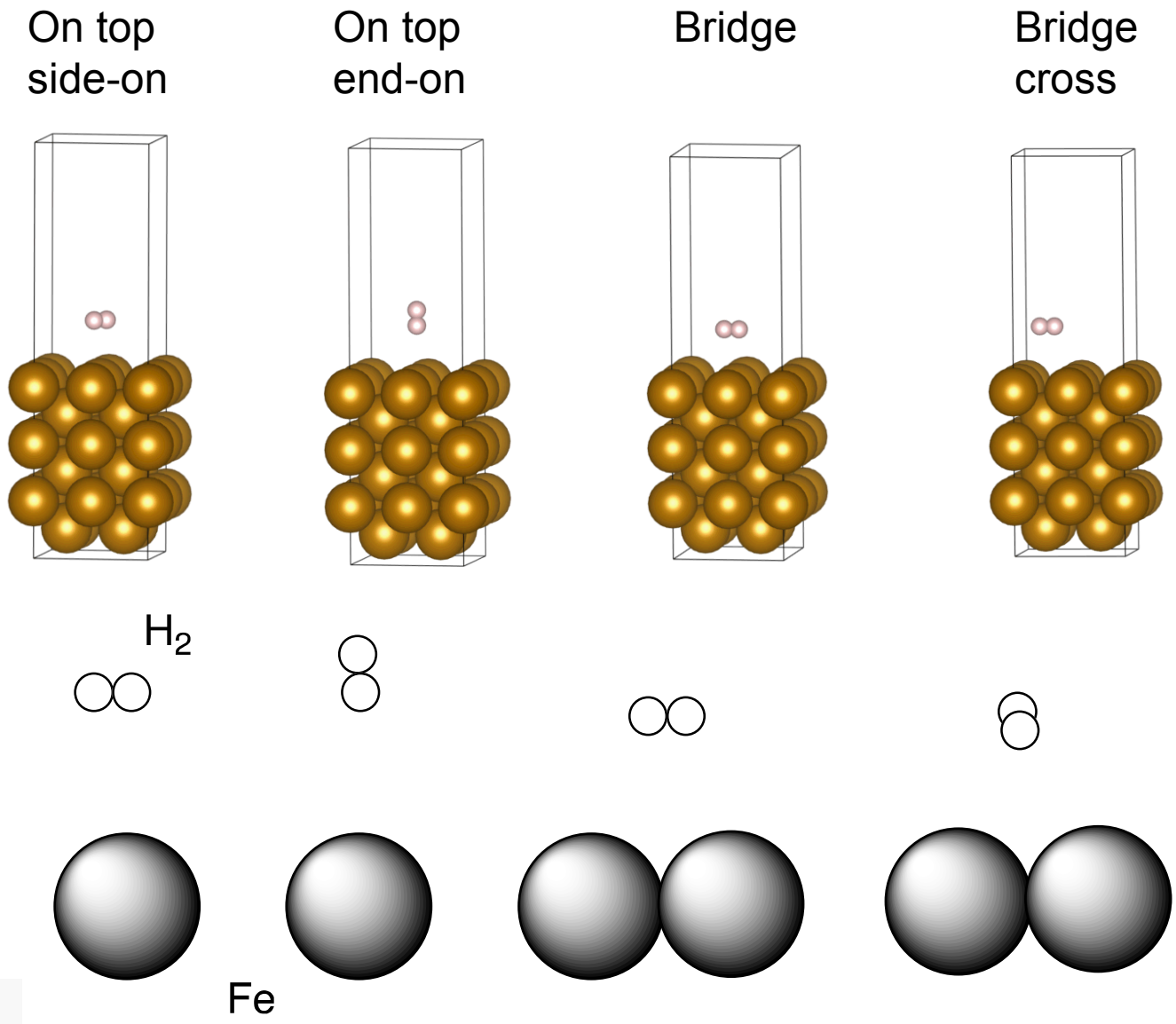

# $H_2$ dissociation on Fe surface

**On top side-on**

trajectory

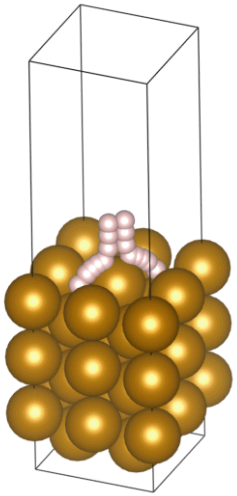

Single $H_2$ molecule approaches the surface in parallel orientation

**Bridge cross**

trajectory

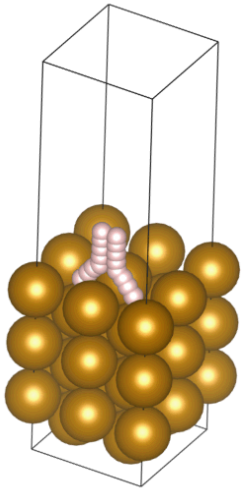

Single $H_2$ molecule approaches the surface in parallel orientation across a bridge site

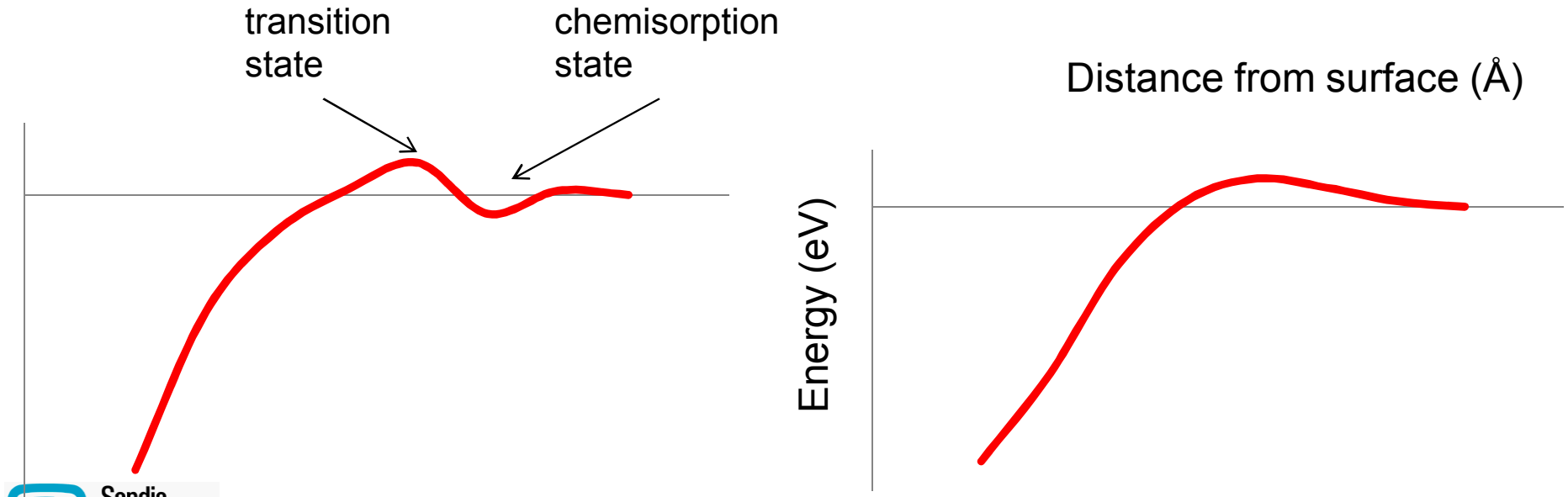


Sandia National Laboratories

# $H_2$-accelerated fatigue crack growth not absolutely inhibited by $O_2$: depends on da/dN and R ratio

B.P. Somerday et al., *Acta Mater*, 2013

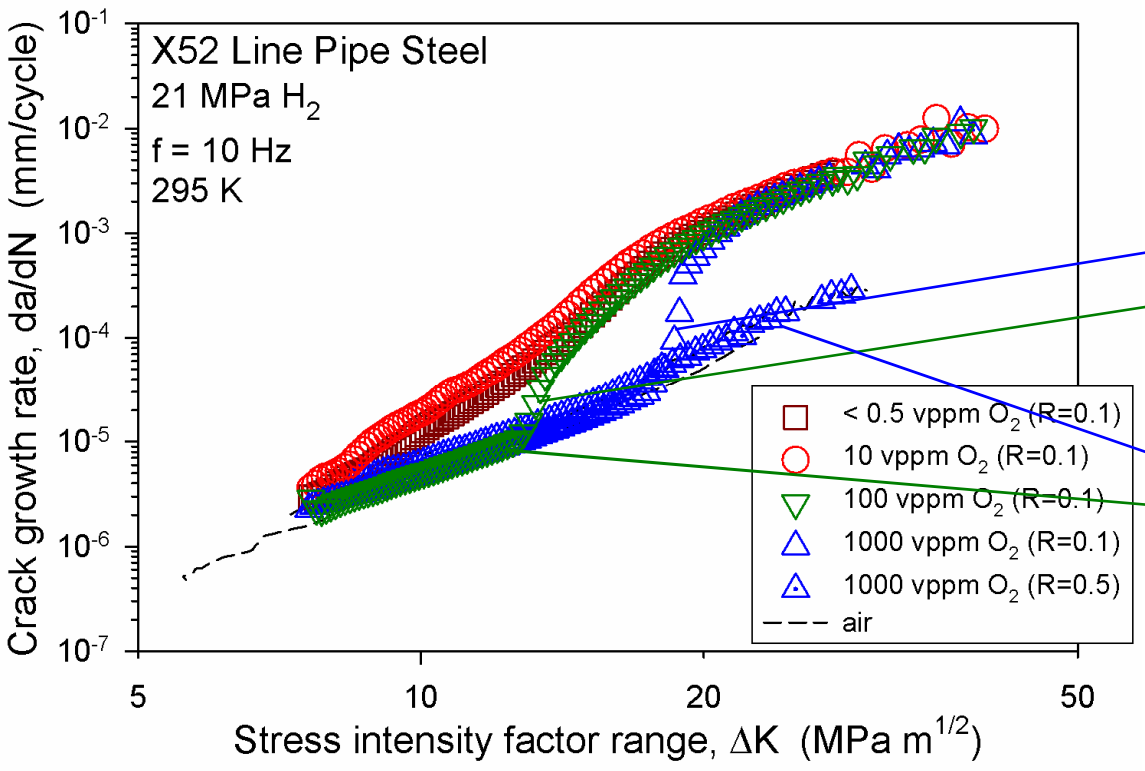


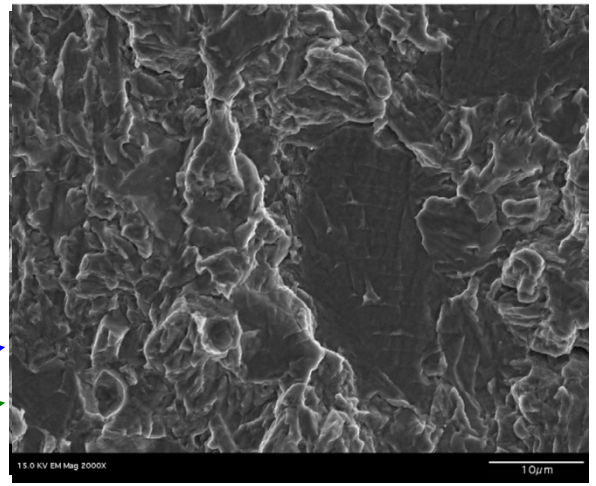

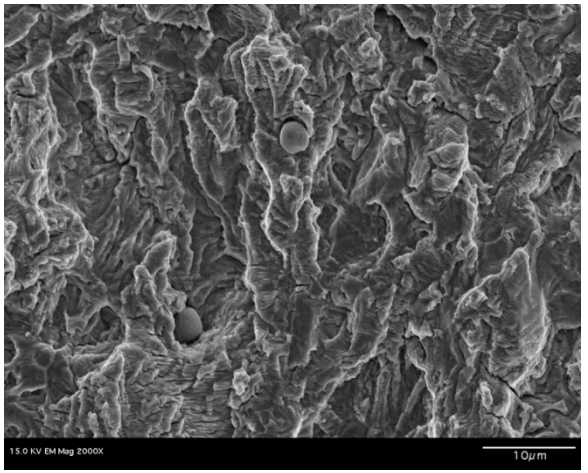

***H-assisted crack path evolves from intergranular to transgranular***

Sandia National Laboratories

# da/dN measured as function of frequency in $H_2$ gas over range of $O_2$ concentrations

B.P. Somerday et al., *Acta Mater*, 2013

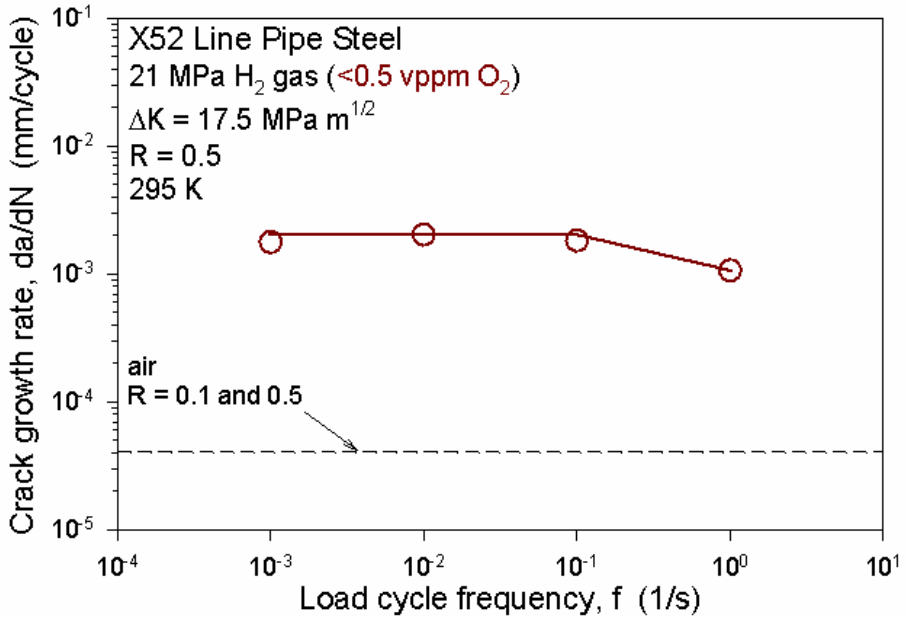


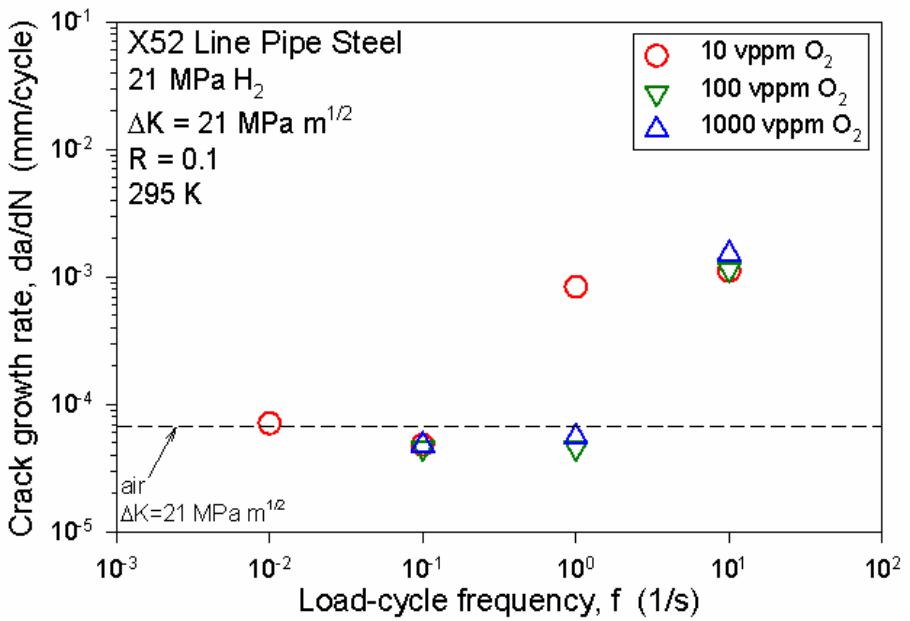


- ***In $H_2$ gas with $O_2$ impurities, da/dN decreases to rates in air as frequency decreases***
- ***Frequency at transition from accelerated da/dN to rates in air depends on $O_2$ concentration***

Sandia National Laboratories

# Model predictions consistent with *da/dN* vs. frequency data measured in $H_2$+$O_2$ gas

B.P. Somerday et al., *Acta Mater*, 2013

$$f\big|_{crit} = \frac{0.3\chi Dp_{tot}(1-\nu^2)}{(da/dN)\pi(z\theta)_{crit}R_gTE\sigma_0}\left(\frac{\Delta K}{\sqrt{a^*}(1-R)}\right)^2$$

$(z\theta)_{crit}$ from measured *da/dN* vs. $\Delta K$ data in $H_2$+100 vppm $O_2$

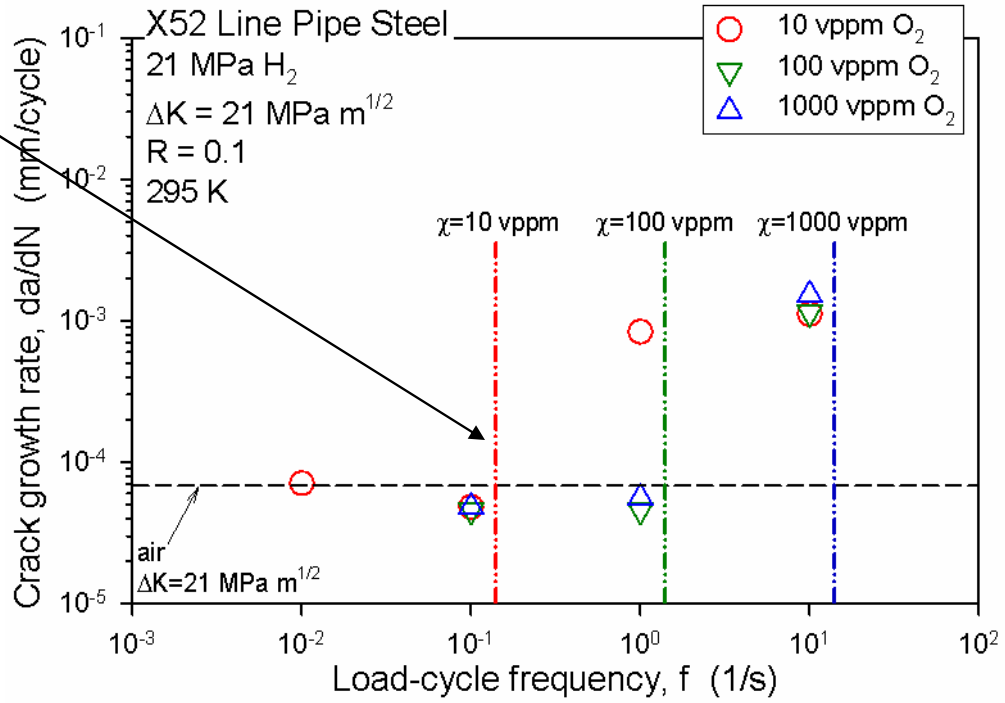


***Predicted frequency for transition to accelerated da/dN consistent with measurements at 10 and 100 vppm $O_2$***

Sandia National Laboratories

# Model can guide interpretation of $H_2$-assisted fatigue crack growth data

Macadre et al., *Engineering Fracture Mechanics*, 2011

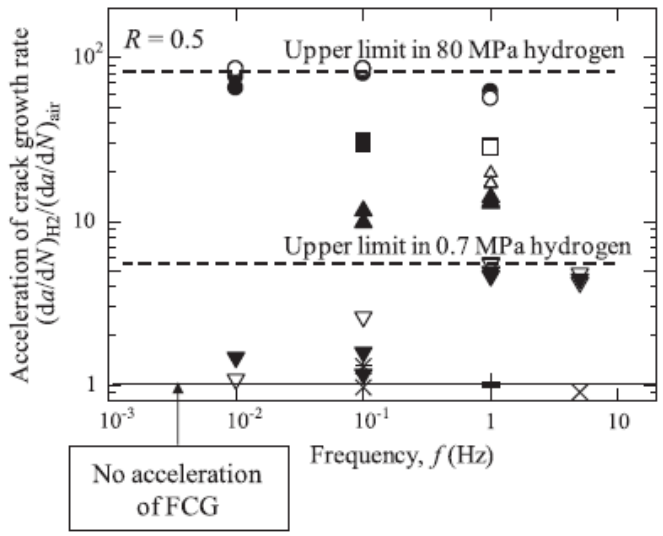


Hydrogen atmosphere

| Specimens | 0.7 MPa | 10 MPa | 40~45 MPa | 90 MPa |
|---|---|---|---|---|
| Circumferential (SCI, SCO) | ▼ | ▲ | ■ | ● |
| Longitudinal (SLI, SLO) | ▽ | △ | □ | ○ |

Nitrogen atmosphere

| Specimens | 0.7 MPa $N_2$ | 90 MPa $N_2$ |
|---|---|---|
| Longitudinal (SLI, SLO) | × | + |

$$f|_{crit} = \frac{0.3\chi Dp_{tot}(1-\nu^2)}{(da/dN)\pi(z\theta)_{crit}R_gTE\sigma_0}\left(\frac{\Delta K}{\sqrt{a^*}(1-R)}\right)^2$$

Stewart, *Mechanisms of Environment Sensitive Cracking of Materials*, 1977

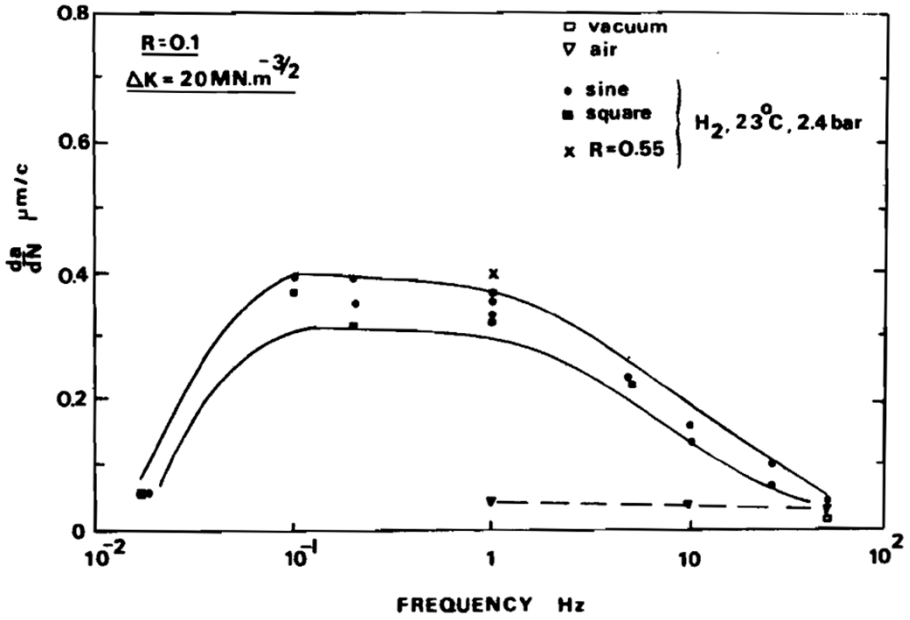


***Model indicates that decreasing da/dN at lower frequency could be attributed to $O_2$ impurities***

Sandia National Laboratories

# Model does not predict onset of accelerated crack growth for high-purity $H_2$ case

$Z_{crit}$ from measured $da/dN$ vs. $\Delta K$ data in $H_2$+100 vppm $O_2$

$$\left.\frac{da}{dN}\right|_{crit} = \frac{0.3\chi Dp_{tot}(1-\nu^2)}{f\pi z_{crit}\theta_O R_g T E \sigma_0}\left(\frac{\Delta K}{\sqrt{a^*}(1-R)}\right)^2$$

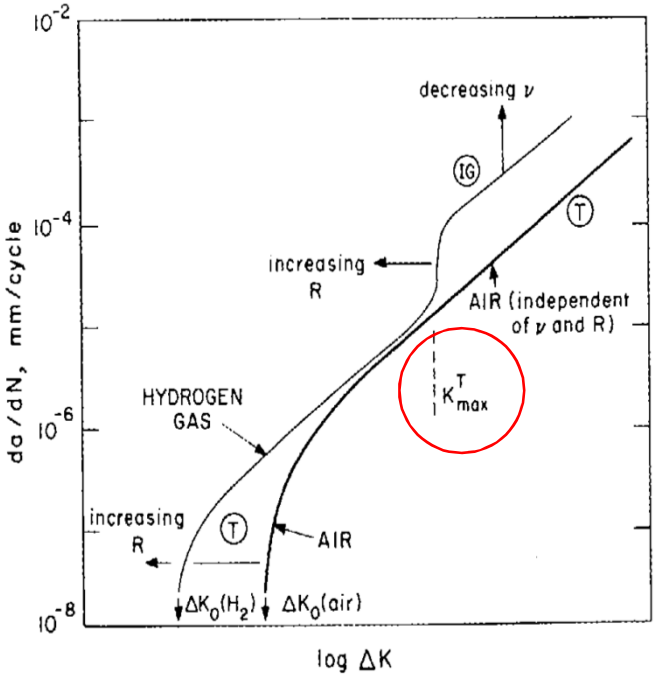


Suresh and Ritchie, *Metal Science*, 1982

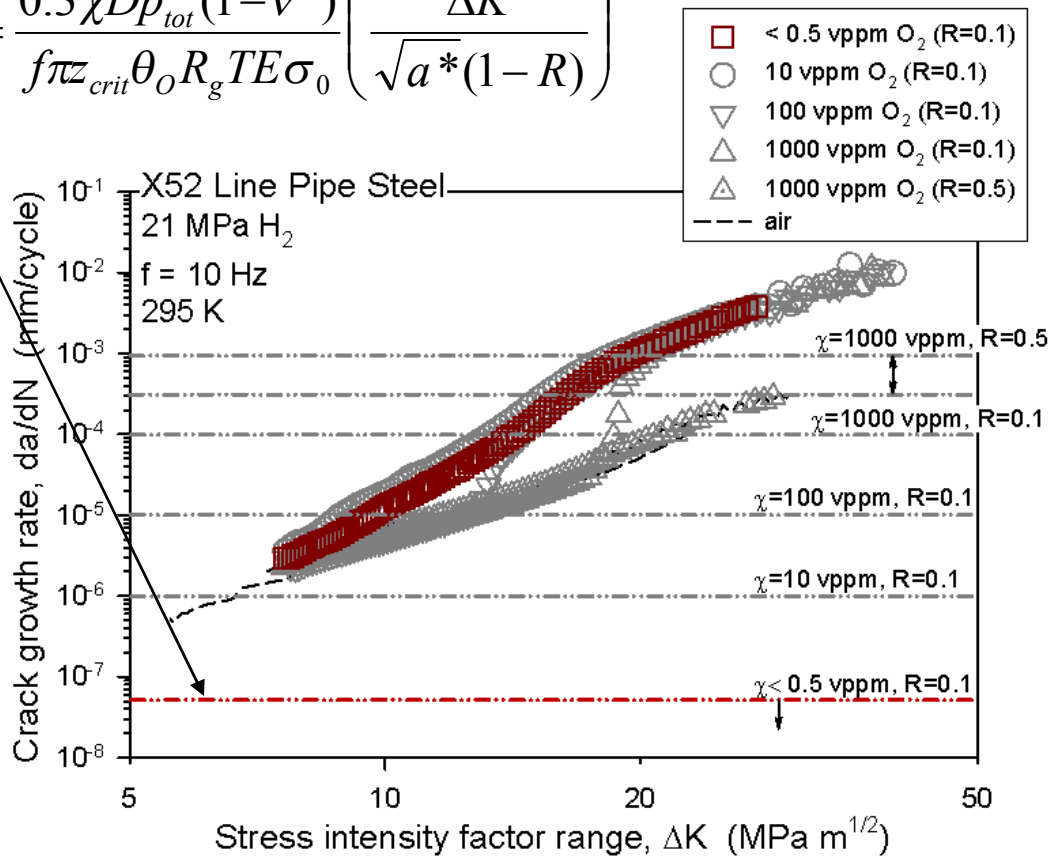


***Rationale: onset of accelerated crack growth dictated by threshold values of both da/dN and $K_{max}$***

B.P. Somerday et al., *Acta Mater*, 2013

Sandia National Laboratories

# Model critically tested by performing fatigue crack growth experiments at lower pressure

- Question: inhibition governed by $O_2$ concentration or absolute $O_2$ partial pressure?
- Results at constant system pressure inconclusive → both concentration and absolute partial pressure vary
- Can isolate partial pressure by varying system pressure at constant $O_2$ concentration
  - Results show no effect on critical *da/dN* for accelerated crack growth
  - Conclusion: inhibition dictated by $O_2$ concentration
- Model predicts governing role of $O_2$ concentration
  - $Dp_{tot}$ term is constant

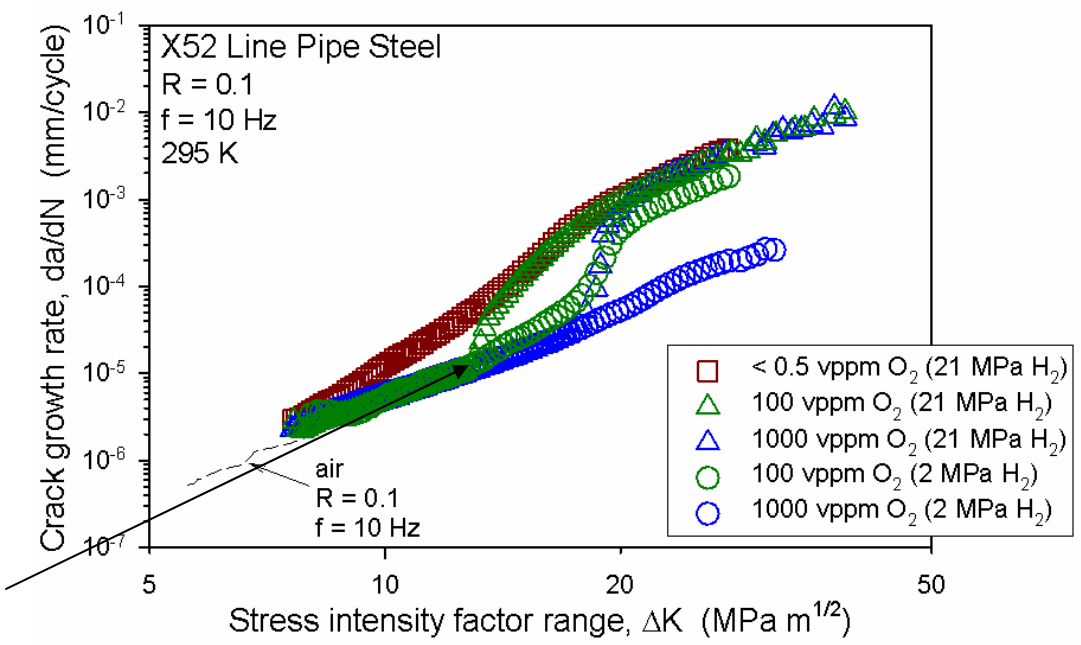


$$\left.\frac{da}{dN}\right|_{crit} = \frac{0.3\chi Dp_{tot}(1-\nu^2)}{f\pi z_{crit}\theta_O R_g TE\sigma_0}\left(\frac{\Delta K}{\sqrt{a^*}(1-R)}\right)^2$$

Sandia National Laboratories

# More advanced model accounts for varying $O_2$ profile in "breathing" crack

B.P. Somerday et al., *Acta Mater*, 2013

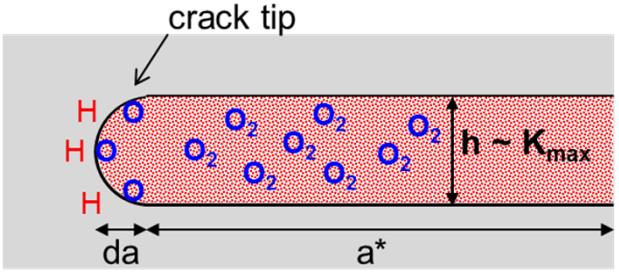


gray-scale shading → oxygen concentration, $c_O$

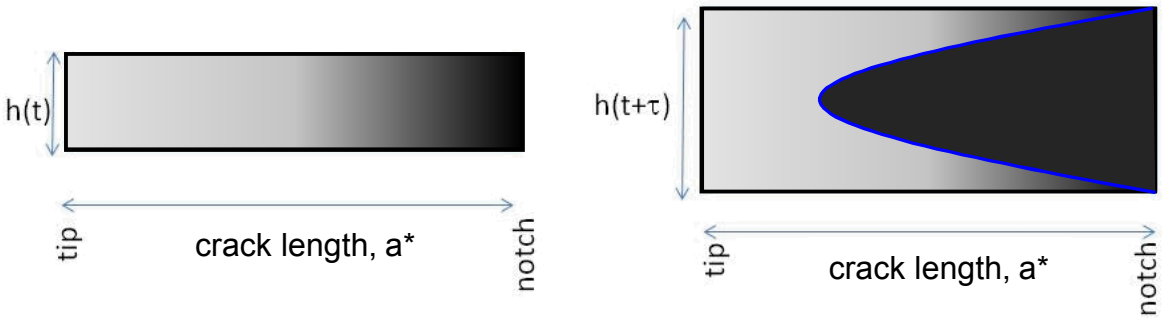


minimum tension

maxmum tension

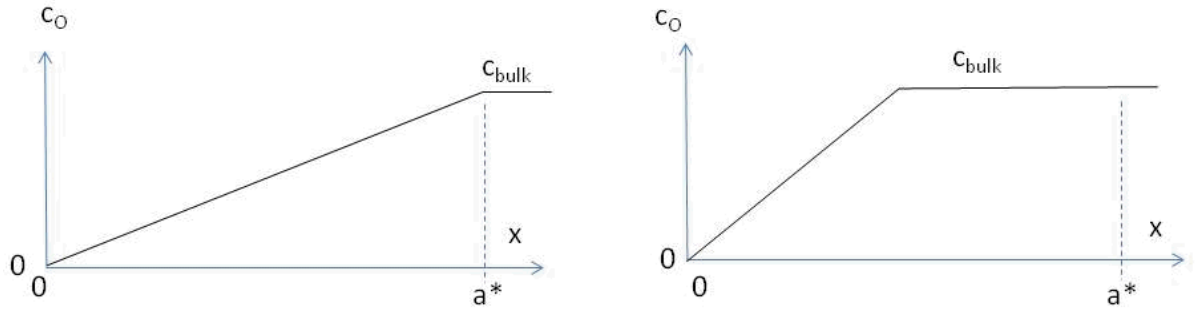


$$S\theta = \frac{0.3\chi D p_{tot}(1-\nu^2)}{(da/dN) f \pi R_g T E \sigma_0 a^*}\bar{h}$$

***Model based on "breathing" crack retains dependence on $O_2$ concentration ($\chi$) and frequency ($f$)***

Sandia National Laboratories